Chinese Chemical Letters 36 (2025) 110070

Contents lists available at ScienceDirect

Chinese Chemical Letters

journal homepage: www.elsevier.com/locate/cclet

Application of magnetic nanomaterials in peptidomics: A review in the past decade

Yimin Guo, Yiting Luo, Shuwen Hua, Chuan-Fan Ding*, Yinghua Yan*

State Key Laboratory for Managing Biotic and Chemical Threats to the Quality and Safety of Agro-products, School of Materials Science and Chemical Engineering, Ningbo University, Ningbo 315211, China

ARTICLE INFO

Article history:
Received 27 January 2024
Revised 28 May 2024
Accepted 29 May 2024
Available online 30 May 2024

Keywords:
Glycosylation
Phosphorylation
Magnetic nanomaterials
Enrichment
Mass spectrometry

ABSTRACT

Protein glycosylation and phosphorylation, as two of the most important protein post-translational modifications (PTMs), play key roles in living organisms. However, glycopeptides and phosphopeptides have low abundance in biological samples. In addition, the low ionization efficiency and the severe signal interference in the presence of other peptides present great difficulties for their direct mass spectrometry (MS) analysis. Therefore, it is important to develop feasible enrichment strategies to pretreat glycopeptides and phosphopeptides in complex samples before MS detection. This paper reviews the application of various magnetic nanomaterials (MNMs) in glycopeptides and phosphopeptides in the last decade, with emphasis on the enrichment principles, the design and synthesis process of the materials, and the effectiveness of the application in biological samples. In addition, possible future trends and potential challenges are presented.

1. Introduction

Protein PTMs include glycosylation, phosphorylation, ubiquitination, methylation, *etc.* [1,2]. Among them, protein glycosylation and phosphorylation are two of the most common and important PTMs and play important roles in various biological processes, such as intercellular signaling, molecular recognition, protein folding, and immune response [3,4]. In general, protein glycosylation and phosphorylation can respond to physiological and pathological conditions in individuals. The development of many diseases is inextricably linked to abnormal protein glycosylation and phosphorylation, such as cancer, neurodegenerative diseases, and rheumatoid arthritis [5-7]. Literature shows that glycosylation and phosphorylation can act not only individually but also synergistically. Alzheimer's disease (AD) is a classic example. It develops as a result of abnormal protein glycosylation and the accelerated hyperphosphorylation of tau proteins, which are in the brain [8]. Therefore, the detection and quantification of glycosylated and phosphorylated proteins and the identification of their corresponding loci are important for diagnosing diseases, understanding pathogenesis, discovering potential disease markers, and developing new drugs [9-11]. MS techniques are popular for their high throughput, efficiency, and speed [12,13]. However, the low ionization efficiency of glycopeptides and phosphopeptides, their low concentration in biological samples, and the complexity of biological samples lead to significant difficulties in direct analysis using MS techniques [14]. Therefore, prior to analyzing glycopeptides and phosphopeptides by MS, it is necessary to pre-treat the samples, *e.g.*, by developing a range of strategies for enriching and separating glycopeptides and phosphopeptides.

Currently, the enrichment strategies for glycopeptides include hydrophilic interaction method (HILIC), boric acid method, hydrazide chemistry, lectin affinity chromatography, *etc.* [15-18]. For the enrichment of phosphopeptides, the strategies include immobilized metal affinity chromatography (IMAC), metal oxide affinity chromatography (MOAC), functionalized amines, *etc.* [19-21]. Based on the different enrichment strategies of glycopeptides and phosphopeptides, a systematic categorization is necessary to introduce them.

MNMs are materials that are size-controlled and externally easy to modify [22,23]. Compared with centrifugation and other methods, MNMs with strong magnetic responsiveness can realize rapid separation, simple operation, time-saving, and meet the requirement of green separation. Moreover, MNMs are non-toxic, easily available, and have good biocompatibility. For the materials themselves, different types of functionalization of MNMs have different enrichment effects. Therefore, the surface of MNMs can be modified in different ways through various connectors to further cus-

* Corresponding authors.
E-mail addresses: dingchuanfan@nbu.edu.cn (C.-F. Ding), yanyinghua@nbu.edu.cn (Y. Yan).

https://doi.org/10.1016/j.cclet.2024.110070
1001-8417/

tomize the framework according to experimental needs. For example, MNMs can form hybrids with graphene, graphene oxide (GO), and other substances to increase the surface area [24,25]. Various functionalized MNMs (*e.g.*, organic frameworks, mesoporous materials, metal oxides) are widely used for the enrichment of glycopeptides and phosphopeptides [26,27]. Currently, there are several reviews on the application of MNMs in peptidomics. In 2020, Zheng *et al.* present strategies for the synthesis of magnetic borate materials and summarize the applications of magnetic borate materials in separation of glycoproteomics and other biomacromolecules [28]. In 2021, Qi *et al.* reviewed the application of magnetic adsorbents for the isolation and enrichment of glycoproteins and glycopeptides in human body fluids [29]. However, there is no review on the enrichment of glycopeptides, phosphopeptides, and both of them simultaneously by MNMs. Summarizing them may be useful for diagnosing diseases and discovering disease markers.

This paper reviews the applications of functionalized MNMs in peptidomics in the last decade based on the advantages of MNMs and the importance of peptidomics. It covers the mechanisms of enrichment and separation of glycopeptides and phosphopeptides by the materials and focuses on summarizing the design and synthesis of these materials, as well as their performance in standard and real samples. In addition, an outlook on the field is provided, and future trends are described.

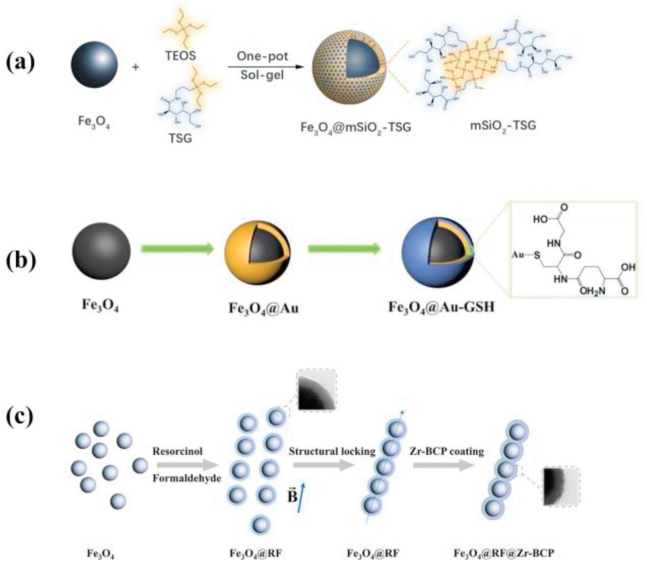

Fig. 1. (a) Preparation of Fe_3O_4@$mSiO_2$-TSG. Reprinted with permission [36]. Copyright 2021, Elsevier B.V. (b) Preparation of Fe_3O_4@Au-GSH. Reprinted with permission [37]. Copyright 2019, Elsevier B.V. (c) Preparation of Fe_3O_4@RF@Zr-BCP. Reprinted with permission [64]. Copyright 2023, Elsevier B.V.

2. Magnetic nanomaterials in glycopeptide analysis and enrichment principles

Glycosylation is one of the typical PTMs of proteins, accounting for more than half of the proteins in living organisms, and plays structural, protective, and stabilizing roles in living cells and participates in biological processes such as protein translation, degradation, immunoprotection, and signal transduction. In other words, protein glycosylation has an important role in organisms. More and more studies have shown that altered or abnormal glycoprotein expression is closely related to many diseases. It is noteworthy that more than 50% of the current clinical disease markers are glycoproteins. However, cancer, neurodegenerative diseases, and other human societies cannot yet be defeated, and their early diagnosis and interventional treatment are particularly important. Therefore, quantitative and qualitative analysis of glycopeptides is of great importance. MNMs have been widely used in the enrichment of glycopeptides, as shown in Table 1. This section describes them according to different enrichment strategies.

2.1. Hydrophilic magnetic nanomaterials

Hydrophilic materials have hydrophilic groups such as hydroxyl, carboxyl, amino, and sulfonic acids. The mechanism of action of the HILIC strategy is the formation of hydrogen bonding and electrostatic interactions between hydrophilic groups on the material and the hydroxyl groups on glycopeptide. HILIC, with its simple reaction conditions, fast and efficient enrichment procedure, and unbiased glycan structure selectivity, is the most widely used strategy [30].

2.1.1. Zwitterionic hydrophilic magnetic nanomaterials

Compared with conventional hydrophilic materials, zwitterionic hydrophilic (ZIC–HILIC) materials have superior hydrophilicity due to the coexistence of positive and negative ions and are more advantageous for enriching glycopeptides. Amino acids are typical. Feng *et al.* first obtained Fe_3O_4 NPs (NPs stand for nanoparticles) by solvothermal reaction, then Fe_3O_4/L-Cys was obtained by coordination of the metal with organic groups (Fe and -SH) [31]. The material has a simple synthesis step and high hydrophilicity. It has excellent sensitivity (2.5×10^{-11} mol/L) and selectivity (HRP:BSA = 1:100) in glycopeptide enrichment. In total, 376 glycopeptides were identified in human serum, corresponding to 393 *N*-glycosylation sites from 118 glycoproteins. With the successful application of Fe_3O_4/CS and Fe_3O_4/GSH (GSH stands for glutathione) in human serum glycosylation analysis, it is shown that these materials provide an efficient and convenient method of material synthesis for glycoproteomics studies. Mesoporous materials with unique pore structure and high surface area have been widely used. For example, Jiang *et al.* prepared ordered mesoporous alumina (OMA) materials for phosphopeptide enrichment [32]. Xu *et al.* utilized mesoporous dopamine with built-in metal-organic frameworks (MMP-b-MOFs) and combined them with MS in order to extract serum fingerprinting profiles of Crohn's disease and healthy individuals [33]. Ma *et al.* constructed copper-ion-immobilized hollow covalent organic frameworks (V-HCOFs@Cu^{2+}) in order to trap the Amyloid beta-peptide 1–42 (Aβ1–42), which is one of the AD disease markers [34]. Mesoporous SiO_2 ($mSiO_2$) greatly enhances the hydrophilicity and specific surface area of the material and has an excellent size exclusion effect. Deng's group successively prepared Fe_3O_4@$mSiO_2$-IDA (IDA stands for iminodiacetic acid), L-Cys-Fe_3O_4@$mSiO_2$, and Fe_3O_4@$mSiO_2$-TSG (TSG represents *N*-(3-triethoxysilylpropyl)glucosamine) (Fig. 1a) [27,35,36]. All these materials were effectively used to enrich *N*-glycopeptides.

GSH is a hydrophilic tripeptide composed of glutamic acid, cysteine, and glycine with richer hydrophilic groups. A good way to prepare GSH as a hydrophilic material is to coordinate the -SH with a metal group. For example, Qi and his colleagues constructed Fe_3O_4@Au-GSH (Fig. 1b) [37]. Sun *et al.* constructed GSH-modified magnetic amphiphilic materials (denoted as Fe_3O_4@TpBD@Au@GSH) [38]. Li's group constructed magnetic nanofibrous materials (denoted as magHN/Au-GSH) [39]. Zhang *et al.* designed Fe_3O_4@TiO_2-GSH [40]. In these materials, Au can enhance the biocompatibility of the materials, and the most important role is to graft GSH.

Combining hydrophilic substances to work simultaneously can greatly enhance the performance of the material. Our group combined GSH and L-Cys to construct composites (denoted as Fe_3O_4–CG) [41]. The long molecular length of GSH means it cannot bind to Fe_3O_4 in large quantities, while L-Cys can reduce

Table 1
Magnetic nanomaterials in glycopeptide analysis.

MNMs	Sensitivity (mol/L)	Selectivity	Samples	Identified peptides	Ref.
Hydrophilic magnetic nanomaterials					
Fe_3O_4/L-Cys	2.5×10^{-11}	1:100	Human serum	376	[31]
L-Cys-Fe_3O_4@mSiO_2	1.0×10^{-9}	1:100	Healthy and gastric cancer human saliva	46, 36	[27]
Fe_3O_4@mSiO_2-IDA	1.0×10^{-9}	1:200	Human serum	424	[35]
Fe_3O_4@mSiO_2-TSG	0.1×10^{-9}	–	Healthy and breast cancer human serum	162, 156	[36]
Fe_3O_4@Au-GSH	1.0×10^{-8}	1:100	–	–	[37]
Fe_3O_4@TpBD@Au@GSH	0.1×10^{-9}	1:2000	Human serum and human saliva	492, 160	[38]
magHN/Au-GSH	2.0×10^{-9}	1:100	Human serum	246	[39]
Fe_3O_4@TiO_2-GSH	0.5×10^{-9}	1:100	HeLa-exosomes and MDA-MB-231-exosomes and MCF-7-exosomes	531, 659, 754	[40]
Fe_3O_4–CG	0.5×10^{-10}	1:5000	Healthy and Alzheimer's disease human serum	131, 180	[41]
Fe_3O_4@CS@Au-L-Cys	0.5×10^{-9}	1:1000	Human serum and saliva	63, 37	[42]
Fe_3O_4-PEI-pMaltose NPs	0.1×10^{-9}	1:100	Human renal mesangial cell tryptic digest	449	[48]
AEK8-maltose functionalized SiO_2@Fe_3O_4 and C@Fe_3O_4 MNPs	0.2×10^{-9}	1:150	Human serum	282	[49]
magMOF@Au-maltose	0.1×10^{-9}	1:200	Human serum	113	[43]
Fe_3O_4@G6P	0.5×10^{-9}	1:100	Human serum and saliva	243, 183	[50]
Mag Zr-MOF@G6P	0.1×10^{-9}	1:200	Healthy and kidney cancer urine	104, 123	[51]
Fe_3O_4@PANI	0.5×10^{-9}	–	N204 and N211 from the serum haptoglobin β chain	63	[53]
Fe_3O_4@SiO_2@PMSA	0.1×10^{-11}	–	Mouse liver	458	[54]
GO/Fe_3O_4/Au/PEG	2.5×10^{-10}	1:100	Human serum	255	[55]
Fe_3O_4@TiO_2@PEG	0.1×10^{-9}	1:100	Human serum	300	[56]
Fe_3O_4@PDA@Zr-SO_3H	0.1×10^{-9}	1:100	Human serum	177	[62]
GO@Fe_3O_4@MOF-303	0.1×10^{-9}	1:1000:1000	Healthy and hepatocellular carcinoma human serum	274, 265	[63]
Fe_3O_4@RF@Zr-BCP	1.5×10^{-8}	1:200	Mouse teratoma cell extracts	97	[64]
Fe_3O_4@TpPa-1	2.8×10^{-8}	1:100	Human serum	228	[66]
Fe_3O_4@SiO_2-aniline	1.1×10^{-6}	1:100	Human serum	148	[67]
MMP	–	1:50	Human serum	356	[68]
Boronic acid-based magnetic nanomaterials					
Fe_3O_4-GO@PAAPBA	–	–	–	–	[69]
Fe_3O_4@SiO_2-BA	–	1:1	–	–	[70]
Fe_3O_4@SiO_2@UiO-PBA	–	–	–	–	[71]
Fe_3O_4@COF-ABB	–	1:1	–	–	[72]
Fe_3O_4@SiO_2/MIPs	–	–	–	–	[73]
Fe_3O_4@pTiO_2@MIP	0.7×10^{-8}	–	–	–	[74]
Hydrazide-based magnetic nanomaterials					
pGMA-H	2.0×10^{-8}	1:100	Mouse liver tissues	511	[77]
Fe_3O_4@PMAH	–	–	Colorectal cancer patient serum	175	[78]
Other magnetic nanomaterials					
GO/Fe_3O_4/PEI/Ag	2.5×10^{-10}	1:100	Human serum	136	[79]

"-": Not mentioned.

the site resistance on the surface of Fe_3O_4. The concatenation of the two solves this problem effectively. The ultra-high hydrophilic Fe_3O_4–CG provides abundant affinity sites for capturing glycopeptides, and the superparamagnetism of magnetic spheres simplifies the separation procedure. The good selectivity (HRP:BSA = 1:5000) and high sensitivity (0.5×10^{-10} mol/L) were outstanding. Recently, a novel probe (denoted as Fe_3O_4@CS@Au-L-Cys) was prepared by combining CS and L-Cys for the first time by Zhao *et al.* [42]. CS contains large amounts of hydroxyl and amino groups. CS provides abundant attachment sites for Au NPs while binding glycopeptides. This created conditions for subsequent grafting of L-Cys. Fe_3O_4@CS@Au-L-Cys shows good potential in complex biological samples and provides a powerful tool for relevant glycoproteomic research.

2.1.2. Carbohydrate-based hydrophilic magnetic nanomaterials

Carbohydrates contain many hydrophilic hydroxyl groups, such as maltose [43], glucose [44], CS [45], and cyclodextrin [46,47], with high hydrophilicity and biocompatibility. In glycoproteomics, the coupling of magnetic substrates with carbohydrates is favored by researchers. For example, the materials modified with maltose, Fe_3O_4-PEI-pMaltose NPs [48], the AEK8-maltose functionalized SiO_2@Fe_3O_4 and C@Fe_3O_4 MNPs [49], and magMOF@Au-maltose [43] were developed successively, and all of them showed excellent performance in glycopeptide enrichment. Taking Fe_3O_4-PEI-Maltose MNPs as an example, Fe_3O_4-PEI MNPs were first obtained by one-pot solvothermal reaction, then 2-bromoisobutyryl bromide (BIB) and triethyl-amine (TEA) were modified to expose the azide group on the surface of Fe_3O_4-PEI, and finally 1 propargyl-O-Maltose was grafted with the azide group by click chemistry. Polyethyleneimine (PEI) has long and branched chains, high functional group density, high hydrophilicity, and easy post-functionalization. Maltose is rich in hydroxyl groups, and the hydrophilicity is greatly enhanced by binding with PEI, achieving superb capture of glycopeptides with an adsorption capacity for IgG (150 mg/g), high sensitivity (0.5×10^{-11} mol/L), and a recovery rate of 85%.

Glucose-6-phosphate (G6P) is essential for the metabolism of life. Li *et al.* used a one-step method to link G6P with Fe_3O_4 (denoted as Fe_3O_4@G6P) [50]. The phosphate group in G6P successfully ligands with Fe^{2+}/Fe^{3+} ions to expose glucose, which contains plenty of hydroxyl groups to trap glycopeptides. The grafting of G6P with Fe_3O_4 utilizes the IMAC strategy (coordination of metal ions with phosphate groups) and imparts a highly hydrophilic surface to the material. The excellent hydrophilicity allowed Fe_3O_4@G6P to have good sensitivity (0.5×10^{-9} mol/L), specificity (1:100), and stability (at least 10 times) in glycopeptide enrichment. They also showed good enrichment in biological samples such as human saliva and serum. Later, Hu *et al.* improved on this basis to prepare Mag Zr-MOF@G6P [51]. Zr-MOF was firstly encapsulated on the surface of Fe_3O_4, which increased the specific surface area and the reaction site for grafting with G6P. Mag Zr-MOF@G6P showed lower detection limit and higher selectivity than Fe_3O_4@G6P.

2.1.3. Polymer-based hydrophilic magnetic nanomaterials

The modification of hydrophilic small molecules on a substrate is monolayer, whereas polymers are multilayered and can be adjusted in thickness with numerous hydrophilic groups on their chains. Therefore, polymeric MNMs usually have higher hydrophilicity than hydrophilic small molecule MNMs [52]. However, the preparation of polymers is tedious, and for this reason, they are not as widely used in proteomics as other materials. Lai *et al.* utilized a magnetic polyaniline material (denoted as Fe_3O_4@PANI) to achieve efficient enrichment of *N*-glycopeptides in complex samples [53]. Under the dual effects of hydrogen bonding and electrostatic adsorption, the enrichment effect of Fe_3O_4@PANI was fast and convenient. In addition, the material is highly stable and easy to prepare, which has great potential for application in the comprehensive enrichment of *N*-glycopeptides. Chen *et al.* first designed Fe_3O_4@SiO_2@PMSA by reflux precipitation polymerization [54]. The thicker polymer coating and abundant amphiphilic groups give Fe_3O_4@SiO_2@PMSA excellent glycopeptide enrichment capabilities, such as ultra-high sensitivity (0.1×10^{-11} mol/L) and loading capacity (100 mg/g). In addition, the material identified 905 specific *N*-glycosylation sites corresponding to 458 *N*-glycoproteins in three parallel experimental analyses of mouse liver extracts. This also indicates the feasibility of this material for detecting low abundance glycopeptides in biological samples.

Polyethylene glycol (PEG) has excellent hydrophilicity, and Jiang *et al.* obtained GO/Fe_3O_4/Au/PEG by functionalizing magnetic GO with SH-PEG for the first time [55]. In this material, SH-PEG enhanced the hydrophilicity, biocompatibility, and binding ability of the material. GO not only has a large specific surface lamellar structure but also abundant hydrophilic groups such as hydroxyl and carboxyl groups. GO/Fe_3O_4/Au/PEG detected 255 glycopeptides from 127 different glycoproteins in human serum. In addition, Deng's group prepared Fe_3O_4@TiO_2@PEG nanoparticles modified by SH-PEG, with TiO_2 protecting the core from the external environment [56]. The excellent magnetic responsiveness gives the material fast separation capability. Similar to GO/Fe_3O_4/Au/PEG, the hydrophilicity of PEG enables Fe_3O_4@TiO_2@PEG to specifically capture glycopeptides. In total, 24 and 33 glycopeptides were identified by MALDI-TOF-MS analysis in the enrichment of HRP and IgG digests, respectively.

2.1.4. Organic frameworks-based hydrophilic magnetic nanomaterials

Organic frameworks are dominated by MOFs and covalent organic frameworks (COFs). Among them, MOFs are a new class of porous coordination polymers made of metal ions or metal clusters ligated with organic ligands, which have the advantages of a large surface area, ultra-high porosity, excellent chemical stability, and easy functionalization [57]. In recent years, they have been utilized in many areas [58-60]. MOFs are easy to obtain, low-cost, and rich in types. They can be used as substrates for subsequent functionalization or grafted onto various carriers, such as graphene and MNMs. Among them, MNMs are attracted to the design of various types of functionalized materials based on them because of their superparamagnetic properties.

Yan's group demonstrated for the first time that MOFs can effectively enrich peptides and exclude macromolecular proteins [61]. Since then, applications of MOFs in proteomics have sprung up. Xie *et al.* constructed sulfonic acid-based functionalized magnetic Zr-MOF materials (denoted as Fe_3O_4@PDA@Zr-SO_3H) [62]. Wang and coworkers reported a magnetic graphene nanoprobe (GO@Fe_3O_4@MOF-303) functionalized with MOF-303 centered on metallic aluminum [63]. In this material, MOF-303 has higher hydrophilicity and hydrolytic stability than other MOFs. The material has a high specific surface area and excellent pore structure, resulting in an ultra-low detection limit (0.1×10^{-9} mol/L) and excellent size exclusion (HRP digest:BSA protein:HRP protein = 1:1000:1000). Moreover, GO@Fe_3O_4@MOF-303 identified 101 glycoproteins corresponding to 274 N-linked glycopeptides from normal human serum and 265 N-linked glycopeptides corresponding to 102 glycoproteins from liver cancer patients. Recently, Gu and coworkers prepared highly hydrophilic magnetic nanochain structured materials (denoted as Fe_3O_4@RF@Zr-BCP) (Fig. 1c) [64]. In three parallel experiments, this material identified 76 glycopeptides corresponding to 72 glycoproteins in 2 μg of mouse teratoma cell extracts. Besides the benefits of MOFs, COFs have strong covalent bonds between their building units, so they have better stability in water [65].

Wang *et al.* constructed magnetic covalent organic framework materials (denoted as Fe_3O_4@TpPa-1) [66]. This material showed remarkable enrichment ability in the analysis of HRP, IgG, and human serum. This also indicates the potential application of COFs in glycoproteomics research.

2.1.5. Other hydrophilic magnetic nanomaterials

The amino group is a very hydrophilic and biocompatible group. Zhang *et al.* introduced the first non-reducing amination reaction to the extraction of *N*-glycopeptides and constructed a novel aniline-functionalized magnetic nanoprobe Fe_3O_4@SiO_2-aniline [67]. In contrast to reductive amination reactions, this method eliminates the need to add reducing agents and desalting after coupling. The enrichment process is simple and less time-consuming compared to hydrazide chemistry. Mesoporous phenolic resins (denoted as MMP) were prepared by Zhang and coworkers with good antioxidant activity, biocompatibility, hydrophilicity, and mesoporous structure [68]. The incorporation of PEI makes MMP more hydrophilic than conventional phenolic resins. Overall, MMP with rich nitrogen-containing functionality and a mesoporous structure showed excellent sensitivity and selectivity in enriching glycopeptides.

2.2. Boronic acid-based magnetic nanomaterials

Boronic acid chemistry is also one of the most widely used methods for glycopeptide enrichment, with the advantages of high enrichment efficiency, good compatibility, and simple operation. Under alkaline conditions, boronic acid can form stable five- or six-membered ring structures with any *cis*-1,2-diol compound, whereas under acidic conditions, the target molecule is released through reversible reactions. Su and coworkers used click chemistry and surface-initiated atom transfer radical polymerization (SI-ATPR) strategy to synthesize a boronic acid-functionalized magnetic nanocomposite probe (Fe_3O_4-GO@PAAPBA) [69]. SI-ATRP not only provides excellent surface grafting density during modification, but also controls the polymer's structure and thickness. Fe_3O_4-GO@PAAPBA has good selectivity for glycoproteins at pH 9.0 and pH 7.4. Moreover, the material has a high adsorption capacity for ovalbumin (OVA) (471 mg/g) and transferrin (Trf) (450 mg/g). Xue and coworkers constructed Fe_3O_4@SiO_2-BA, whose recognition ability was confirmed when selectively enriched glycoproteins from hybrid systems containing Trf and cytochrome c (Cyt C) [70]. Li *et al.* synthesized Fe_3O_4@SiO_2@UiO-PBA through a new bifunctionalized magnetic metal-organic framework (Fig. 2a) [71]. The presence of amino groups increased the hydrophilicity of the material. Fe_3O_4@SiO_2@UiO-PBA has a high binding capacity for glycoproteins at pH 7.4, such as OVA of 327.28 mg/g, Trf of 241.17 mg/g, and HRP of 530.79 mg/g. Chen's group constructed Fe_3O_4@COF-ABB by combining boric acid groups on Fe_3O_4@COF surface [72]. The combined action of COF and benzeneboronic acid resulted in excellent selectivity and binding ability for the material.

Molecular imprinting is an effective means of preparing adsorbent materials. Molecularly imprinted polymers (MIPs) can provide tailored binding sites for target molecules, and their binding to borates can be used to trap glycopeptides. Guo *et al.* prepared novel imprinted materials (named Fe_3O_4@SiO_2/MIPs) (Fig. 2b) [73]. In this material, borate groups bind OVA, then dopamine self-polymerizes on the material surface, and finally the OVA is removed to form a cavity. Fe_3O_4@SiO_2/MIPs have specific recognition of target molecules. Sun and coworkers prepared Fe_3O_4@pTiO_2@MIP [74]. Porous TiO_2 (pTiO_2) has a larger surface area, providing more binding sites for subsequent template formation. Compared with Fe_3O_4@SiO_2/MIPs, Fe_3O_4@pTiO_2@MIP has better affinity for glycoproteins.

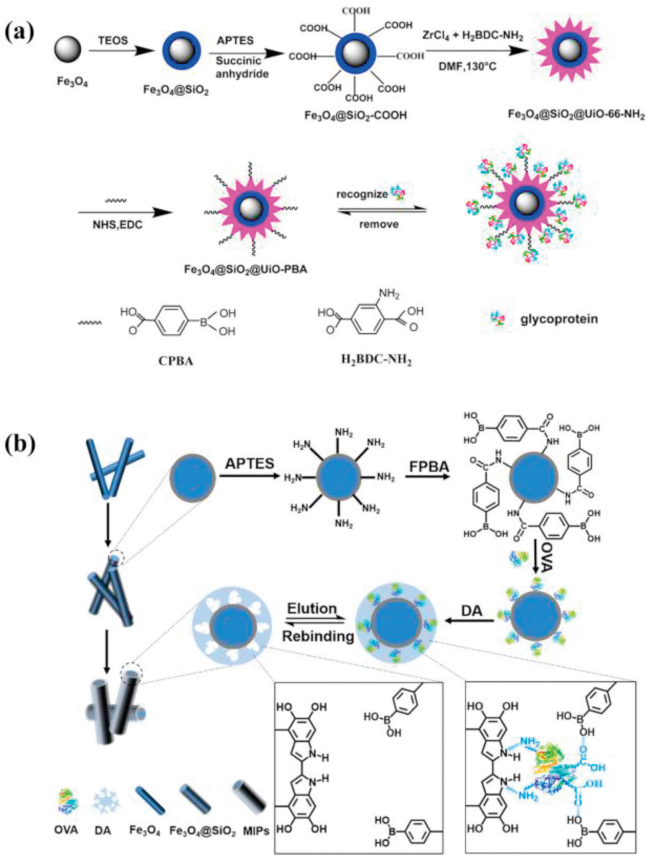

Fig. 2. (a) Preparation of Fe_3O_4@SiO_2@UiO-PBA. Reprinted with permission [71]. Copyright 2018, American Chemical Society. (b) Synthesis of Fe_3O_4@SiO_2/MIPs. Reprinted with permission [73]. Copyright 2022, Elsevier Inc.

2.3. Hydrazide-based magnetic nanomaterials

Because of this, hydrazide chemistry has a better enrichment specificity of up to 90% compared to other methods [75,76]. In 2003, Zhang *et al.* used this method for the first time to enrich glycoproteins in human serum. Conventional hydrazide-functionalized materials are limited and monolayered for the loading of hydrazide groups because of their small surface area. This suggests that it is necessary to increase the loading of the material for the hydrazide moiety to achieve efficient capture of glycopeptides. To improve the modification density of hydrazine functional groups on the material surface, Cao *et al.* synthesized multivalent hydrazide functionalized particles using the SI-ATRP technique (denoted as pGMA-H) [77]. The surfaces of these particles have a hydrazide group density three times higher than that of conventional hydrazide functionalized materials. Liu *et al.* constructed a methacrylhydrazine (PMAH)-functionalized magnetic nanocomposite (denoted as Fe_3O_4@PMAH) [78]. Fe_3O_4@PMAH showed better sensitivity than commercially available hydrazine resin, with a more than five-fold improvement in signal-to-noise ratio. In addition, in total, 175 glycopeptides, attributed to 63 glycoproteins, were identified in the sera of colon cancer patients. However, hydrazide chemistry has shortcomings, such as the long sample processing time and the step of $NaIO_4$ oxidizing the hydroxyl group, destroying the polysaccharide structure, resulting in the failure to elucidate the polysaccharide structure.

2.4. Other magnetic nanomaterials

Apart from the most common MNMs mentioned above, Jiang *et al.* constructed Ag NPs-functionalized magnetic GO composite

nanoprobes (denoted as GO/Fe_3O_4/PEI/Ag) [79]. Among them, PEI acts as a reducing and stabilizing agent for Ag NPs and the amine group rich in its chain can enhance the hydrophilicity of the material. The Ag NPs bind to the hydroxyl groups on the glycopeptide through multivalent interactions, and the mechanism is similar to the HILIC model. Therefore, the PEI and Ag NPs in this material act synergistically with HILIC and multivalent interactions to capture the glycopeptide. GO/Fe_3O_4/PEI/Ag showed high specificity (1:100) in enriching glycopeptides. In addition, the special two-dimensional (2D) structure reduces the enrichment time to one minute, and material stability of up to one month.

2.5. Comparison of glycopeptide enrichment methods

Overall, the methods for enriching glycopeptides each have superior points. The mechanism of action of the HILIC strategy is the formation of hydrogen bonding and electrostatic interactions between hydrophilic groups on the material and the hydroxyl groups on glycopeptide. The reaction conditions are simple, and the enrichment process is fast and efficient, but the selectivity is low. The principle of boric acid chemistry is that under alkaline conditions, boronic acid can form stable five- or six-membered ring structures with any *cis*-1,2-diol compound, whereas under acidic conditions, the target molecule is released through reversible reactions. Boronic acid chemistry has the advantages of high enrichment efficiency, compatibility, and simplicity of operation, but has low specificity and is susceptible to non-target inhibition. Hydrazide chemistry is similar to boronic acid chemistry in that both react with the polyhydroxyl structure on the sugar chain. The difference is that hydrazide chemistry requires oxidizing the hydroxyl group on the glycopeptide to an aldehyde group by $NaIO_4$ and then reacting the hydrazide group with the aldehyde group to form a hydrazone. The method is highly specific, but the glycan structure is easily damaged by oxidizing agents (*e.g.*, $NaIO_4$).

3. Magnetic nanomaterials in phosphopeptide analysis and enrichment principles

Protein phosphorylation, which is achieved by modifying one or more phosphate groups on proteins, plays an important role in a variety of cellular processes, including metabolism, growth, differentiation, and apoptosis [80]. It is estimated that there are about 700,000 potential phosphorylation sites in eukaryotic cells and that phosphorylation usually occurs on T, S, and tyrosine (Y) residues in a ratio of about 200:1800:1 [81]. Proteins can have single or multiple phosphorylation sites, and phosphorylation is complex and a rapid and reversible means of regulating protein activity and signaling. Therefore, the regulation of phosphorylation is relevant to the onset and progression of disease. Comprehensive analysis of the dynamic process of protein phosphorylation and accurate localization of phosphorylation sites are of great significance in peptidomics. At present, MNMs have found wide application in peptidomics, as shown in Table 2.

3.1. Magnetic IMAC-based nanomaterials

IMAC is one of the most widely used strategies and can be combined with many ligands (such as phosphate, arsenate, PDA, adenosine triphosphate (ATP)) to immobilize metal ions [82-85]. The fundamental principle of IMAC enrichment of phosphopeptides is the coordination reaction between phosphate groups and metal ions. Under acidic conditions, the metal ion can chelate with the phosphate group by bridging dienes, and under alkaline conditions, the captured phosphopeptides are released. The following is an introduction to the classification of ligands.

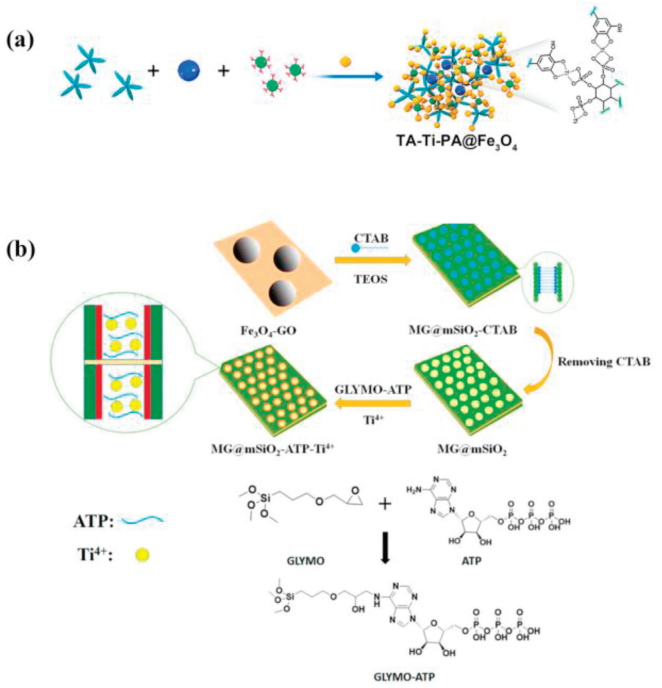

Fig. 3. (a) Preparation of TA-Ti-PA@Fe_3O_4. Reprinted with permission [87]. Copyright 2021, Elsevier B.V. (b) Synthesis of MG@mSiO_2-ATP-Ti^{4+}. Reprinted with permission [98]. Copyright 2018, American Chemical Society.

3.1.1. Phosphate ligands-based magnetic nanomaterials

IDA and NTA (NTA stands for nitrilotriacetic acid) are the traditional acidic chelating ligands, both of which have polycarboxylate groups [86]. However, the interaction between metal ions and carboxyl groups is weak, which leads to easy loss of metal ions as well as much lower enrichment efficiency. Compared with carboxyl groups, phosphate groups have stronger coordination with metal ions. Therefore, the development of phosphoric acid-based materials has received attention from researchers.

Both tannic acid (TA) and phytic acid (PA) have strong metal coordination abilities. Xie's group immobilized Ti^{4+} in conjunction with PA and TA to obtain TA-Ti-PA@Fe_3O_4 (Fig. 3a) [87]. Due to the high affinity sites of TA and PA, the material surface is highly loaded with Ti^{4+}. In the enrichment of standard samples, TA-Ti-PA@Fe_3O_4 exhibited high selectivity (β-casein:BSA = 1:1000). In addition, a total of 3408 phosphopeptides were identified in rat liver lysates tryptic digests, which showed better enrichment compared to commercial TiO_2 and Fe^{3+}-IMAC kits. After that, Zhang's group used PA as a linker to connect the two metals to construct Fe_3O_4@UiO-66-NH_2@PA-Ti^{4+} [88]. With the combined effect of Zr-O clusters and Ti^{4+}, complemented by strong hydrophilicity, Fe_3O_4@UiO-66-NH_2@PA-Ti^{4+} showed satisfactory exosome enrichment ability. There were 348 and 284 proteins identified in complex samples (cell culture medium and urine exosomes), respectively. Also, rapid isolation of structurally intact exosomes from complex biological agents due to specific interactions between metals and exosomal phospholipid bilayers indicates that the material shows great potential for enrichment of isolated exosomes related to complex biological samples, providing support for future work. Yan's group designed novel magnetic nanoparticles (denoted as Fe_3O_4@mSiO_2@APA@Ti^{4+}/Nb^{5+}) immobilized with bimetallic ions [89]. In this material, 3-glycidoxypropyltrimethoxysilane (GLYMO) was utilized to connect Fe_3O_4@mSiO_2 with aminomethylphosphonic acid (APA). The connection to APA provided ample opportunities for Ti^{4+} and Nb^{5+} immobilization. The prepared na-

Table 2
Magnetic nanomaterials in phosphopeptide analysis.

MNMs	Sensitivity (mol/L)	Selectivity	Samples	Identified peptides	Ref.
Magnetic IMAC-based nanomaterials					
TA-Ti-PA@Fe_3O_4	4.0×10^{-11}	1:1000	Rat liver lysate	3408	[87]
Fe_3O_4@UiO-66-NH_2@PA-Ti^{4+}	–	–	Cell medium and urine	348, 284	[88]
Fe_3O_4@mSiO_2@APA@Ti^{4+}/Nb^{5+}	0.5×10^{-12}	1:1500	Serum and saliva	4, 24	[89]
Fe_3O_4@mPDA@Ti^{4+}	0.1×10^{-9}	1:200	Human saliva	38	[90]
Ti^{4+}-ATP-NPs	3.0×10^{-12}	1:5000	Rat liver mitochondria	406	[96]
Ga^{3+}-ATP MNPs	3.0×10^{-11}	1:5000	Rat liver mitochondria	193	[97]
MG@mSiO_2-ATP-Ti^{4+}	2.0×10^{-11}	1:1000	Nonfat milk digest and human saliva and serum	13, 19 and 4	[98]
ZrAs-Fe_3O_4@SiO_2	0.1×10^{-9}	1:100	Human serum	4	[99]
TiO_2/MHMSS and ZrAs–Fe_3O_4@SiO_2	–	–	HL60 cells	8281	[100]
Fe_3O_4-mag@Gd^{3+}	0.5×10^{-12}	1:5000	Non-fat milk and human saliva and serum	12, 11, 4	[101]
Fe_3O_4@TAPTDHTA-Ti^{4+}	0.5×10^{-10}	1:5000	Nonfat milk and human serum and human saliva	9, 3333, 4	[102]
Magnetic MOAC-based nanomaterials					
Fe_3O_4@mZrO_2	7.6×10^{-11}	1:1000	Spiked protein digests and tumor cell lysates	–	[106]
Fe_3O_4-TiNbNS	2.0×10^{-10}	1:100	Leukemia patient sera	4	[107]
MC-TiNbNS	2.0×10^{-10}	1:200	Skim milk and human serum	10, 8	[108]
Fe_3O_4/GO	2.5×10^{-11}	1:1:100	Nonfat milk and human serum	15, 4	[112]
magG/(Ti-Sn)O_4	4.0×10^{-11}	1:1500	Mouse brain	170	[113]
Fe_3O_4/g-C_3N_4/MoO_3	0.1×10^{-11}	1:1:5000	Non-fat milk and human serum and saliva and A549 cell lysate	7, 58, 108, 10	[114]
Fe_3O_4@H-*f*TiO_2	0.2×10^{-9}	1:10,000	HeLa cell extracts	1485	[115]
Fe_3O_4@H-TiO_2@*f*-NiO	2.0×10^{-10}	1:5000	HeLa cell extracts	972	[116]
Fe_3O_4@TiO_2-ZrO_2@mSiO_2	0.2×10^{-12}	1:1000:1000	Human saliva	30	[117]
MSNs	–	1:100	Nonfat milk	7	[120]
Fe_3O_4@TiO_2@Lys-MIPs	0.2×10^{-9}	1:100:100	Human serum and urine	2, 2	[121]
PMNP	0.1×10^{-6}	–	–	–	[122]
Fe_3O_4@G-ZIF-8	1.0×10^{-11}	1:200	Human saliva and serum	25, 14	[126]
Fe_3O_4@SiO_2@Ce-Zr-MOF@PA	0.1×10^{-9}	1:800	Non-fat milk and human serum and human saliva	19, 4, 15	[127]
Fe_3O_4@ZIF-8@Zn-Ga LDH	0.1×10^{-11}	1:5000	Skimmed milk, human saliva and serum	13, 324, 122	[128]
Magnetic nanomaterials combination of IMAC and MOAC					
DZMOF	0.7×10^{-10}	1:5000	Human saliva	17	[129]
DFMMOF	5.0×10^{-11}	1:1000	Human serum and nonfat milk	4, 15	[130]
mMOF-FBP-Ti^{4+}	0.2×10^{-9}	1:1:500	Non-fat milk and human saliva	14, 14	[131]
Fe_3O_4@nSiO_2@mSiO_2/TiO_2-Ti^{4+}	4.0×10^{-8}	1:50	Nonfat milk	15	[132]
T2M	0.1×10^{-9}	1:800	Non-fat milk and human saliva and healthy eye lens and cataract lens	23, 4, 658, 162	[133]
Magnetic amino-based nanomaterials					
Fe_3O_4/PDA/PAMA-Arg	0.2×10^{-11}	1:500	Nonfat milk and rat brain lysate	14, 1059	[134]
Fe_3O_4@LDH@NH_2-GAA	0.1×10^{-11}	1:5000	Nonfat milk and human saliva and serum and A549 cell lysates	16, 15, 4, 11	[135]
Fe_3O_4@NH_2@ZIF-90@Car	0.1×10^{-11}	1:500	Nonfat milk and human serum and saliva	17, 3, 28	[136]
Ti_3C_2Tx@PAMAM@Fe_3O_4	1.0×10^{-9}	1:800	Nonfat milk and human serum and human saliva and rat brain lysate	24, 19, 4, 1705	[137]

"-": Not mentioned.

nomicrospheres have a large specific surface area (151.1 m^2/g) and a good chelating ability for bimetals. The material exhibited excellent sensitivity (0.5×10^{-12} mol/L), excellent selectivity (β-casein:BSA = 1:1500, maximum mass ratio) and excellent loading capacity (330 mg/g) in enriching phosphopeptides.

3.1.2. PDA ligands-based magnetic nanomaterials

Dopamine can be polymerized into polydopamine under mild conditions. Polydopamine is favored by researchers for its easy accessibility, high hydrophilicity, and good biocompatibility. Because of its rich neighboring phenolic hydroxyl group, it can chelate various metal ions more easily, such as Ti^{4+} [90], Nb^{5+} [91,92], Hf^{4+} [93]. Fe_3O_4@mPDA@Ti^{4+} was prepared by Xu *et al.* [90]. In their work, the magnetic mPDA core-shell structure was first prepared by the soft template method, and then Ti^{4+} was chelated on to obtain the material. Moreover, Deng's group also immobilized eight metals (including Nb^{5+}, Ti^{4+}, Zr^{4+}, Ga^{3+}, Y^{3+}, In^{3+}, Ce^{4+}, and Fe^{3+}) on PDA surface (named Fe_3O_4@PDA-Mn^+) and made a systematic comparison [94]. Different metal ions have different coordination abilities, and thus the materials exhibit different capturing abilities for phosphopeptides.

3.1.3. ATP ligands-based magnetic nanomaterials

ATP is an indispensable molecule in living organisms and plays an important bioregulatory function in cells [95]. ATP contains three phosphate groups, which provide a richer set of chelating active sites compared to the usual phosphate ligands. In addition, the presence of purine bases and ribose increases hydrophilicity and has the potential to reduce the non-specific adsorption of non-phosphorylated peptides. Therefore, ATP has great potential in the preparation of IMAC materials. Zhang *et al.* designed a novel magnetic nanoparticle (denoted as Ti^{4+}-ATP-NPs) [96]. ATP acts as a chelating ligand to immobilize Ti^{4+}. Ti^{4+}-ATP-NPs showed high specificity (β-casein:BSA = 1:5000), sensitivity (3.0×10^{-12} mol/L), and superb adsorption capacity (1046.5 mg/g) in enriching phosphopeptides. In protein studies of rat liver mitochondria, the material showed better performance than commercial TiO_2. Later, Zhang *et al.* prepared Ga^{3+}-ATP MNPs with slight modifications [97]. Ga^{3+} has better binding ability for polyphosphopeptides than Ti^{4+} and allows rapid, specific identification of monophosphopeptides in complex biological samples, especially polyphosphopeptides. Sun *et al.* developed ATP-Ti^{4+}-modified magnetic mesoporous graphene composites (MG@mSiO_2-ATP-Ti^{4+}) (Fig. 3b) [98]. The combination of GO and mSiO_2 has a large substrate-specific surface area and good size exclusion effect. As a feasible functionalized material, MG@mSiO_2-ATP-Ti^{4+} was successfully enriched for low-abundance phosphopeptides in biological samples.

3.1.4. Arsenate ligands-based magnetic nanomaterials

In the periodic table of elements, As and P belong to the same fourth main group and have similar properties. So similarly, arsenate has good coordination abilities as well as phosphate. IMAC materials with phosphate as a linker have been widely used in phosphopeptide enrichment. Based on this, arsenate also has the

potential to be used as an efficient linker. However, not much literature has been reported in this area so far. In 2011, Feng's group reported the first successful use of zirconium arsenate-modified magnetic nanoparticles (denoted as ZrAs-Fe_3O_4@SiO_2) for specific capture of phosphopeptides [99]. After that, they prepared TiO_2-coated magnetic SiO_2 nanospheres (denoted as TiO_2/MHMSS) [100]. They were used together with the previous ZrAs-Fe_3O_4@SiO_2 for sequential enrichment and identification of phosphopeptides, and were found to possess complementary capabilities. After combining strong cation exchange chromatography (SCX) and sequential solid phase extraction techniques, the enriched phosphopeptides were analyzed by LC-MS/MS, and 11,579 unique phosphorylation sites corresponding to 3432 phosphoproteins of HL60 cells were identified. Although arsenate-related magnetics have not been reported in phosphoproteomics, their potential remains non-negligible and needs to be further developed.

3.1.5. Other ligands-based magnetic nanomaterials

Magadiite consists of one or more negatively charged SiO_4 sheets with a large specific surface area and strong corrosion resistance. Magadiite nanosheets have a special 2D layered structure and abundant affinity sites, which can be used as adsorbents to remove heavy metal ions. Jiang *et al.* pioneered the design of magadiite composites for phosphopeptide analysis (denoted as Fe_3O_4-mag@Gd^{3+}) [101]. To simplify the operation, Fe_3O_4 NPs were introduced into this material. The abundant affinity sites and effective adsorption space make the material effective in phosphopeptide analysis. Fe_3O_4@TAPTDHTA-Ti^{4+} composites with magnetic bifunctional COF-immobilized Ti^{4+} were prepared by He *et al.* The neighboring hydroxyl group on COF in Fe_3O_4@TAPTDHTA-Ti^{4+} provides a large number of active sites for Ti^{4+} coordination [102]. Moreover, the combination of high specific surface area and mesoporous structure allowed the material to exhibit excellent performance towards phosphopeptides, such as high sensitivity (0.5×10^{-10} mol/L), selectivity (β-casein:BSA = 1:5000), and size exclusion effect (β-casein tryptic digest:β-casein:BSA = 1:250:250). Fe_3O_4@TAPTDHTA-Ti^{4+} has been well used in complex biological samples, including tryptic digests of skimmed milk, human serum, and human saliva. More importantly, 3333 phosphopeptides from 1409 phosphoproteins corresponding to 3492 phosphorylation sites were clearly identified from tryptic digests of HeLa cell lysates.

3.2. Magnetic MOAC-based nanomaterials

MOAC is another of the most widely used strategies in phosphopeptide enrichment. It is based on the mechanism that metal cations are chemically bonded to oxygen-negative ions in the form of M-O. Unlike IMAC, such a binding mechanism makes the metal ion binding stable and less likely to be lost. Metal oxides are not only resistant to high temperatures but also to general pH. Most of them can be both Lewis acids and Lewis bases. In addition, the metal oxides themselves can capture phosphopeptides, or they can be further combined with other substances to obtain modified materials with more complete properties.

3.2.1. Magnetic MOs

Pure MOs have long been applied in the study of phosphopeptides, but the surface area of MOs is too small to meet the research requirements. In addition, magnetic substances not only simplify the synthesis and enrichment processes but even provide certain active sites. Therefore, it is important to develop magnetic MO materials with large surface area and more active sites for phosphoproteomics research. Generally, magnetic MOs are prepared by MOs directly deposited and wrapped on the core surface or by SiO_2, C, PMAA, *etc.* as linkers and then post-synthesis

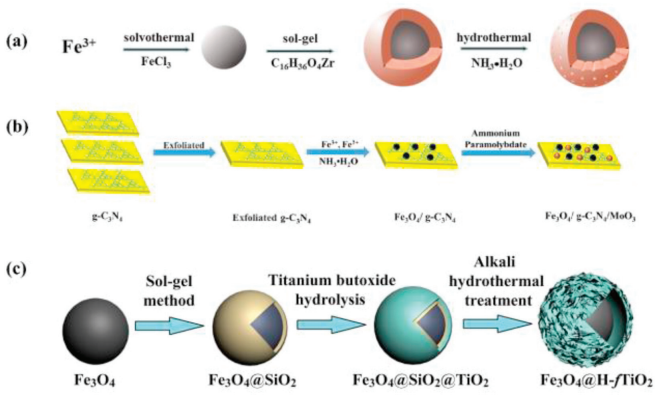

Fig. 4. (a) Preparation of Fe_3O_4@mZrO_2. Reprinted with permission [106]. Copyright 2020, Elsevier. (b) Synthesis of Fe_3O_4/g-C_3N_4/MoO_3. Reprinted with permission [114]. Copyright 2022, Elsevier B.V. (c) Synthesis of Fe_3O_4@H-*f*TiO_2. Reprinted with permission [115]. Copyright 2018, Elsevier B.V.

[103-105]. Mesoporous MOs have excellent properties due to their unique pore structure. Gao *et al.* designed the selective enrichment of phosphopeptides with the mesoporous core-shell structure of Fe_3O_4@mZrO_2 (Fig. 4a) [106]. In their work, Fe_3O_4@mZrO_2 exhibited effective enrichment of monophosphopeptides and polyphosphopeptides and achieved detection limits down to femtomole levels for the target phosphopeptides. Chen *et al.* constructed an embedded magnetic titanium titanate nanosheet using a simple cation exchange method (denoted as Fe_3O_4-TiNbNS) [107]. This 2D nanosheet provides a large surface area and sizable microenvironment. Fe_3O_4 prevents repacking between nanosheets, creating a larger surface area for the material as a whole. It was shown that the material outperforms spherical, layered metal oxides, and reconstituted nanosheets. Moreover, Min *et al.* obtained a ternary magnetic nanocomposite (denoted as MC-TiNbNS) by electrostatic assembly and an *in-situ* growth strategy [108]. The addition of CeO_2 enhances the specific recognition of phosphopeptides by the material. Dephosphorylation activity can be generated by varying the degree of CeO_2 coverage on the sheet, producing a continuously adjustable signal intensity for the phosphopeptide and its dephosphorylation label.

3.2.2. Graphene and carbon-based magnetic nanomaterials

Graphene and carbon-based nanomaterials have the advantages of ultra-high specific surface area, abundant active sites, and nonspecific adsorption and are widely used as substrates in MOAC materials. Magnetic ferrites such as Fe_3O_4, $MnFe_2O_4$, and $ZnFe_2O_4$ have been applied in phosphopeptide enrichment. However, for the current study, the main focus is on the functionalization of Fe_3O_4, and there are fewer studies on the rest of the magnetic materials. These magnetic materials are easy to agglomerate into large particles, and the surface area and dispersibility are subsequently reduced [109-111]. Graphene and carbon-based nanomaterials can be introduced into them to solve this problem. For example, Lian's group prepared Fe_3O_4 nanoparticles using a mild organic molecule-assisted method that is simple and does not require additional additives [112]. Then, Fe_3O_4 was homogeneously immobilized on GO sheets with ultrasound assistance. GO has a large number of carboxyl and hydroxyl groups and is highly biocompatible. Therefore, Fe_3O_4/GO performs well for capturing hydrophilic peptides.

In addition, it is possible to derive MOs materials based on graphene and carbon-based nanomaterials. Deng's group integrated bimetallic oxides ((Ti-Sn)O_4) on the surface of Fe_3O_4/graphene for the first time at the atomic scale to obtain

magG/(Ti-Sn)O_4 [113]. This material concentrates each advantage: Large surface area, superparamagnetism, abundant binding sites, *etc.* It was shown that magG/(Ti-Sn)O_4 containing binary metals exhibited better performance than monometallic magG/TiO_2, magG/SnO_2, and mixtures of both. Among them, the good capture ability for both mono- and polyphosphopeptides also indicates that the combined multi-metal approach is highly promising.

The dispersion of MoO_3 in water is poor, and a better approach is to immobilize it on a particular substrate. The 2D-layered material graphite nitride (g-C_3N_4) has the advantages of large surface area, high adsorption capacity, easy availability, and its own ability to capture phosphopeptides. Combining MoO_3 with g-C_3N_4 not only improves the dispersibility of MoO_3 but also brings out the synergistic enrichment ability of both for phosphopeptides. Fe_3O_4/g-C_3N_4/MoO_3 was prepared by Jiang *et al.* (Fig. 4b) [114]. Ultimately, the material exhibited high specificity (α-casein/β-casein/bovine serum albumin, 1/1/5000), sensitivity (0.1×10^{-9} mol/L), and reproducibility (10 cycles).

3.2.3. SiO_2-based magnetic nanomaterials

SiO_2 has unique physicochemical properties and has played an indispensable role in various fields since its first preparation by the "Stöber method" in 1968. Among them, SiO_2 has the advantages of controllable structure, good aqueous dispersion, and easy modification, which make it a powerful bridge for derivatization and have a significant impact on phosphopeptide enrichment. mSiO_2 is a substrate material for the MOAC strategy because of its large specific surface area and reasonable pore structure. Hong *et al.* designed Fe_3O_4@H-*f*TiO_2 with an egg yolk shell flower-like structure (Fig. 4c) [115]. Firstly, SiO_2 was coated on the core surface by Stöber sol-gel method, and then a TiO_2 layer was formed on the Fe_3O_4@SiO_2 surface by hydrothermal method. During the alkaline hydrothermal process, SiO_2 and TiO_2 were etched, and the SiO_2 layer formed voids to increase the surface area, and the smooth TiO_2 layer was epitaxially formed into nanosheets, whose mesoporous structure could also increase the binding efficiency to phosphopeptides. Fe_3O_4@H-*f*TiO_2 exhibits ultra-high selectivity (α-casein:BSA = 1:10,000) and sensitivity (0.2×10^{-9} mol/L) in phosphopeptide enrichment. Because of the more comprehensive enrichment performance of bimetals than monometals, Hong *et al.* also prepared a bimetallic oxide composite (denoted as Fe_3O_4@H-TiO_2@*f*-NiO) in which TiO_2 was used as the inner shell layer and NiO as the outer shell layer [116]. The flower-like structure of NiO provided spacious space to facilitate phosphopeptide enrichment and elution and basically did not affect the performance of the inner TiO_2 layer. With the synergistic effect of NiO, the material exhibited better enrichment than Fe_3O_4@H-*f*TiO_2, and 135 more phosphopeptides than Fe_3O_4@H-*f*TiO_2 were identified in the extracts of HeLa cells. In addition, Deng's group constructed a binary metal mesoporous composite Fe_3O_4@TiO_2-ZrO_2@mSiO_2, which not only has superparamagnetic properties but also an ordered mesoporous structure and showed a better effect on global phosphopeptides than single metal Fe_3O_4@TiO_2@mSiO_2 and Fe_3O_4@ZrO_2@mSiO_2 under the joint action of bimetals [117]. In addition, the narrow pore size of mSiO_2 can exclude large-sized proteins and allow small-sized peptides to penetrate for good size exclusion.

3.2.4. MIP-based magnetic nanomaterials

MIPs with advantages such as stable structure and specific selective recognition functions are created by molecular imprinting technology and are synthetic mimics that can be used as antibodies or enzymes [118]. They have been used in several fields, such as disease diagnosis, isolation, bioimaging. In general, MIPs are prepared by epitope blotting, surface blotting, and metalization blotting [119]. MIPs excel at the specific capture of phosphopeptides in the presence of specially designed recognition sites. For example, Chen and colleagues developed a novel mesoporous material (MSNs) suitable for small charged molecules by concatenating mSiO_2 and MIPs, demonstrating for the first time the effectiveness of mesoporous MIPs in proteomics [120]. Deng's group used magnetic TiO_2 as a substrate to bind to lysozyme (Lys) through Ti-O in metal oxides and then added a layer of PDA to increase the hydrophilicity of the material. Finally, Lys was stripped out as a mimic and formed a certain cavity (denoted as Fe_3O_4@TiO_2@Lys-MIPs) [121]. The cavity structure is spacious and not easily deformed, providing enough space for the material to specifically capture phosphopeptides. It has excellent properties such as a low detection limit (0.2×10^{-9} mol/L) and high selectivity (Lys:BSA:β-casein = 1:1000:100) in the recognition of standard proteins. Xie's group prepared magnetic nanospheres (PMNP) by epitope blotting using phenyl phosphate as a template, in which TiO_2-functionalized microspheres and SiO_2 were coated in the outermost layer to form the final adsorbent [122]. The recognition capacity of PMNP reached 90.3 μg/mg when it specifically captured tyrosine (pTyr) at very low levels in cells, and the adsorption efficiency was significantly improved and the enrichment time was shortened.

3.2.5. MOF-based magnetic nanomaterials

Based on the excellent properties of MOFs, such as their large specific surface area, excellent structural stability, and tunable pore size, MOFs also have outstanding performance in phosphopeptide enrichment. Many one- or two-component MOF materials have been used [123-125].

Zhang *et al.* first designed Fe_3O_4@ZIF-8 wrapped by ZIF-8 and then grafted the guanidine-acetic acid (GA) on the carboxyl group and Zn grafting to obtain the product (denoted as Fe_3O_4@G-ZIF-8) (Fig. 5a) [126]. The unsaturated affinity site on ZIF-8 and the additional affinity site provided by the guanidine group form a dual action, which greatly enhances the phosphopeptide trapping effect. The material exhibits a large specific surface area (382.5 m^2/g), satisfactory sensitivity (1.0×10^{-11} mol/L), and fast magnetic separation ability (41.6 emu/g). On the whole, the above material illustrates that mounting MOF layers on the surface of magnetic nanoparticles is an effective method for identifying phosphopeptides in complex biological samples, showing the great potential of such materials in proteomics. Wu's group constructed a PA-functionalized bimetallic MOF material, Fe_3O_4@SiO_2@Ce-Zr-MOF@PA [127]. Mesoporous Ce-MOF is more conducive to peptide adsorption than microporous Zr-MOF. PA has six phosphate groups, which can easily form adherence on metal surfaces. Therefore, in this material, PA not only protects the acting groups of the material from damage but also reduces the nonspecific adsorption of non-phosphorylated peptides. In other words, the functionalization of PA improves the enrichment performance of binary MOF nanospheres.

2D layered double hydroxide (LDH) consists of an anionic layer and a metal hydroxide layer. The metal hydroxide layer has a high surface positive charge and is excellent for the capture of negatively charged phosphopeptides. However, 2D LDH are usually buried with affinity sites and have a reduced specific surface area. To compensate for these deficiencies, Qi *et al.* combined LDH with a three-dimensional (3D) template, followed by a MOF-mediated synthesis strategy with a large number of exposed active sites of Zn and Ga on the surface, resulting in a final product (denoted as Fe_3O_4@ZIF-8@Zn-Ga LDH) with a high enrichment efficiency for phosphopeptides in biological samples [128]. A total of 324 phosphopeptides out of 236 phosphoproteins and 122 phosphopeptides out of 79 phosphoproteins were identified by LC-MS/MS in human saliva and serum, respectively.

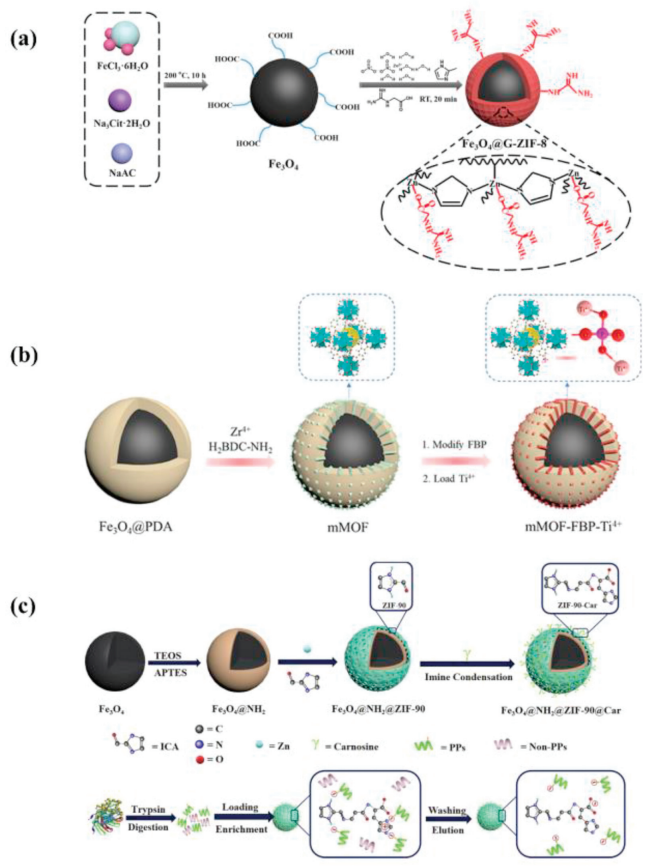

Fig. 5. (a) Preparation of Fe_3O_4@G-ZIF-8. Reprinted with permission [126]. Copyright 2022, American Chemical Society. (b) Synthesis of mMOF-FBP-Ti^{4+}. Reprinted with permission [131]. Copyright 2022, Elsevier B.V. (c) Synthesis of Fe_3O_4@NH_2@ZIF-90@Car. Reprinted with permission [136]. Copyright 2021, Elsevier B.V.

3.3. Magnetic nanomaterials combination of IMAC and MOAC

IMAC and MOAC, as the two most dominant methods in phosphopeptide enrichment at present, are quite mature in their individual applications. Among them, IMAC prefers to capture polyphosphorylated peptides because of the longer amino acid sequence of polyphosphorylated peptides, so that hydrophilicity and basicity are enhanced. On the contrary, the monophosphorylated peptide has a shorter sequence, but it is favored by MOAC. In other words, complete phosphopeptide enrichment cannot be achieved using either of these strategies. The sequential elution strategy has made some progress in the identification of full phosphopeptides, but the method is time-consuming, and there is also the process of multiple transfers that increases the risk of phosphopeptide loss. Therefore, combining IMAC and MOAC and jointly exploiting their respective advantages to develop new functionalized materials is a reliable option to promote full phosphopeptide enrichment. Magnetic UiO-66-NH_2 was bound to Zr^{4+} and Ti^{4+} to obtain DZMOF and DFMMOF, respectively [129,130]. Both of them are centered on bimetals and have better binding ability than pure UiO-66-NH_2. Among them, DZMOF showed an excellent level of specific adsorption in the capture of β-casein (β-casein:BSA = 1:5000). In addition, Gao *et al.* mmobilized Ti^{4+} on 1,6-bisphosphate-modified magnetic Zr-MOF (denoted as mMOF-FBP-Ti^{4+}) (Fig. 5b) [131]. This material unites MOAC, IMAC, and HILIC, which not only targets global phosphopeptide capture but also reduces non-specific adsorption, making it a promising candidate for phosphoproteome analysis. In addition to MOFs, conventional metal oxides are also good candidates. For example, Yang *et al.* developed novel bimetallic magnetic mesoporous nanoparticles (denoted as Fe_3O_4@nSiO_2@mSiO_2/TiO_2-Ti^{4+}) [132]. Among them, mSiO_2 endows the material with high specific surface area, providing more opportunities for different forms of metallotitanium to capture global phosphopeptides. Ultimately, the nanoparticles were enriched with seven monophosphopeptides and eight polyphosphopeptides in skim milk, which showed a more comprehensive enrichment effect than single IMAC or MOAC methods. Wang *et al.* designed Ti^{4+}-immobilized GLYMO-ATP-modified magnetic TiO_2 (denoted as T2M) [133]. The superiority was demonstrated by standard proteins and biological samples. The successful synthesis of T2M provides convenience and more possibilities for the interpretation of diseases associated with phosphoproteomics. In summary, the development of novel nanomaterials for IMAC and MOAC concatenation has become a new research hotspot, which provides more support for the subsequent development of phosphoproteomics.

3.4. Magnetic amino-based nanomaterials

The amino group has good biocompatibility and can react with aldehyde, carboxyl, and imidazole groups, which can be used as a reliable linker to build various materials. The excellent hydrophilicity allows it to interact hydrophilically with phosphate groups and play a unique role in phosphopeptide separation and enrichment. Luo *et al.* prepared magnetic nanoparticles modified with arginine (Arg) (denoted as Fe_3O_4/PDA/PAMA-Arg) [134]. The material was obtained under a single modification of PDA, 2-aminoethyl methacrylate (AMA), and Arg. PAMA-Arg-brushes provide a larger space, creating more opportunities for intermolecular specific recognition. Most importantly, the synergistic effect of the guanidine group and amino group enhances the specificity and sensitivity of the material. Moreover, Jiang *et al.* constructed guanidinoacetic acid-modified magnetic layered hydroxide composites (denoted as Fe_3O_4@LDH@NH_2-GAA) [135]. The material not only has metal ions (Cu^{2+} and Ga^{3+}) on LDH but also contains a large number of guanidine groups, which makes it rich in active sites. Not only that, it also has a high specific surface area due to its laminar structure. Fe_3O_4@LDH@NH_2-GAA exhibits high selectivity (β-casein:BSA = 1:5000) and sensitivity (0.1×10^{-11} mol/L) under the combined action of IMAC and HILIC. Qi *et al.* designed a carnosine (Car) functionalized magnetic MOF composite (denoted as Fe_3O_4@NH_2@ZIF-90@Car) (Fig. 5c) [136]. Car contains carboxyl groups and imidazole, which are key to the affinity interaction with amines. And the presence of ZIF-90 provides the material with a highly specific surface and unique pore structure. Polyamidoamine (PAMAM) has a large number of amino groups. MXenes are novel 2D materials with large surface area and easy-to-change conformations. Yu *et al.* designed a novel magnetic material (denoted as Ti_3C_2Tx@PAMAM@Fe_3O_4) by combining PAMAM with MXenes [137]. The material proved its reliable utility in phosphoproteomics in various dimensions.

3.5. Comparison of phosphopeptide enrichment methods

Overall, phosphopeptide enrichment methods have their own advantages and disadvantages. The fundamental principle of IMAC enrichment of phosphopeptides is the coordination reaction between phosphate groups and metal ions. Under acidic conditions, the metal ion can chelate with the phosphate group by bridging dienes, and under alkaline conditions, the captured phosphopeptides are released. MOAC is based on the mechanism by which metal cations are chemically bonded to oxygen-negative ions in the form of M-O. Unlike IMAC, such a binding mechanism makes

the metal ion binding stable and less likely to be lost. Metal oxides are not only resistant to high temperatures but also to general pH. But both utilize the ligand effect of the metal with the phosphate group and may have incomplete elution. In addition, the amino functionalization method has a better elution effect due to its reversible binding to the target peptide.

4. Magnetic nanomaterials in both glycopeptide and phosphopeptide analysis

Although many magnetic nanoparticles have been widely used to enrich glycopeptides and phosphopeptides, there are still a few for simultaneous enrichment. With the development of peptidomics, simultaneous enrichment is an inevitable trend. Therefore, finding methods to enrich glycopeptides and phosphopeptides at the same time is of great significance for peptidomics research. Based on the different enrichment strategies of glycopeptides and phosphopeptides, how to combine them to construct novel materials and realize the simultaneous enrichment of both is the interest of researchers. The materials used for simultaneous enrichment are shown in Table 3.

For example, the boronic acid method was combined with MOAC. The boronic acid group enriches glycopeptides, and the metal oxide enriches phosphopeptides. Both act separately to achieve simultaneous enrichment. Xu *et al.* have successively designed two magnetic nanocomposites (denoted as TiO_2@SiO_2-$B(OH)_2$@Fe_3O_4@TiO_2 and Fe_3O_4@Au-$B(OH)_2$@$mTiO_2$) in which boric acid groups and TiO_2 are used for simultaneous enrichment [138,139]. In the synthesis of sandwich-shaped nanosheets TiO_2@SiO_2-$B(OH)_2$@Fe_3O_4@TiO_2, the boric acid moiety was introduced into it with the help of SiO_2, and its structure was separated from the TiO_2 layer, avoiding interference with the phosphorylated peptide enrichment. Moreover, in the synthesis of Fe_3O_4@Au-$B(OH)_2$@$mTiO_2$, Fe_3O_4 was encapsulated three times, then tetrabutyl titanate was added to obtain Fe_3O_4@PDA@Au@RF@$mTiO_2$, followed by removal of the organic layer by calcination, and finally 4-mercaptophenylboronic acid was introduced *via* Ti-SH (Fig. 6a). When these two materials were used for simultaneous enrichment, Fe_3O_4@Au-$B(OH)_2$@$mTiO_2$ was enhanced over TiO_2@SiO_2-$B(OH)_2$@Fe_3O_4@TiO_2 in terms of selectivity for enrichment of glycopeptides (HRP:BSA = 1:100) and sensitivity (8.0×10^{-11} mol/L) of phosphorylated peptides.

Based on the fact that HILIC is the most dominant enrichment strategy for glycopeptides, the most dominant method for simultaneous enrichment is still the combination of HILIC and phosphopeptide enrichment strategies, such as IMAC and MOAC. To realize the combination of HILIC and IMAC, Deng's group first obtained Fe_3O_4@PDA@Au (FPA) by conventional methods and then prepared an efficient nanoprobe (FPA@Ti^{4+}@L-Cys) by immobilizing L-Cys (Au) and Ti^{4+} (PDA) sequentially in two routes [140]. As they expected, the material exhibited efficient simultaneous enrichment performance in standard proteins and real samples (mouse brain digest, normal human, and cataract patient lens). Hong *et al.* prepared magnetic graphene nanocomposites functionalized with Ti^{4+} and PA (denoted as MagG@PEI@PA-Ti^{4+}) [141]. PEI with excellent hydrophilicity carries many positive charges, which facilitates the grafting of negatively charged PA. The unique structure and hydrophilicity make PA an ideal chelating substance for Ti^{4+}. The large specific surface area, high hydrophilicity, and Ti^{4+} loading of this material all contribute to its excellent performance in the enrichment of glycopeptides and phosphopeptides.

TiO_2, as the most commonly used material for MOAC strategy, can be combined with many hydrophilic substances. Sun *et al.* immobilized MSA on the magnetic $mTiO_2$ surface to obtain Fe_3O_4@$mTiO_2$_MSA [142]. $mTiO_2$ has higher crystallinity, surface area, and loading capacity. The excellent magnetic responsiveness allowed easy separation of the material. A total of 327 phosphopeptides and 65 glycopeptides were identified in human

Table 3
Magnetic nanomaterials in both glycopeptide and phosphopeptide analysis.

MNMs	Sensitivity		Selectivity		Samples	Identified peptides		Ref.
	G (mol/L)	P (mol/L)	G	P		G	P	
TiO_2@SiO_2-$B(OH)_2$@Fe_3O_4@TiO_2	2.3×10^{-9}	8.7×10^{-10}	1:50	1:50	–	–	–	[138]
Fe_3O_4@Au-$B(OH)_2$@$mTiO_2$	2.0×10^{-9}	8.0×10^{-11}	1:100	1:1000	–	–	–	[139]
FPA@Ti^{4+}@L-Cys	1.0×10^{-9}	0.1×10^{-9}	–	–	Mouse brain, human eye lens of cataract and normal	864, 69, 30	850, 12, 58	[140]
MagG@PEI@PA-Ti^{4+}	5.0×10^{-10}	1.0×10^{-10}	1:1000	1:5000	HeLa cell extract	393	574	[141]
Fe_3O_4@$mTiO_2$-MSA	1.0×10^{-9}	5.0×10^{-11}	1:100	1:800	Human saliva	65	327	[142]
Fe_3O_4@TiO_2-IDA	0.9×10^{-10}	2.8×10^{-10}	1:100	1:800	Mouse brain	330	550	[143]
Fe_3O_4@TiO_2@$mSiO_2$-TSG	1.0×10^{-9}	0.1×10^{-9}	1:200	1:200	Human saliva	94	164	[144]
Fe_3O_4@PDA@MIL-125@Au@L-Cys	0.1×10^{-9}	0.1×10^{-9}	1:100	1:100	Tryptic digests human crystalline lens proteins	81	175	[145]
Fe_3O_4@MIL-100(Fe)	0.1×10^{-9}	0.1×10^{-9}	1:20	1:50	Human saliva	39	43	[146]
Fe_3O_4@SiO_2@(Zr-Ti-MOF)$_{10}$–NH_2	1.0×10^{-9}	1.0×10^{-9}	1:50	1:2000	Rat brain	141	918	[147]
Fe_3O_4@ILI-01@Ti^{4+}	0.1×10^{-11}	0.5×10^{-11}	1:500	1:5000	Human serum	83	122	[148]
Fe_3O_4@HOF	2.0×10^{-10}	4.0×10^{-10}	1:1000	1:1000	Human serum	340	223	[149]

"-": Not mentioned.

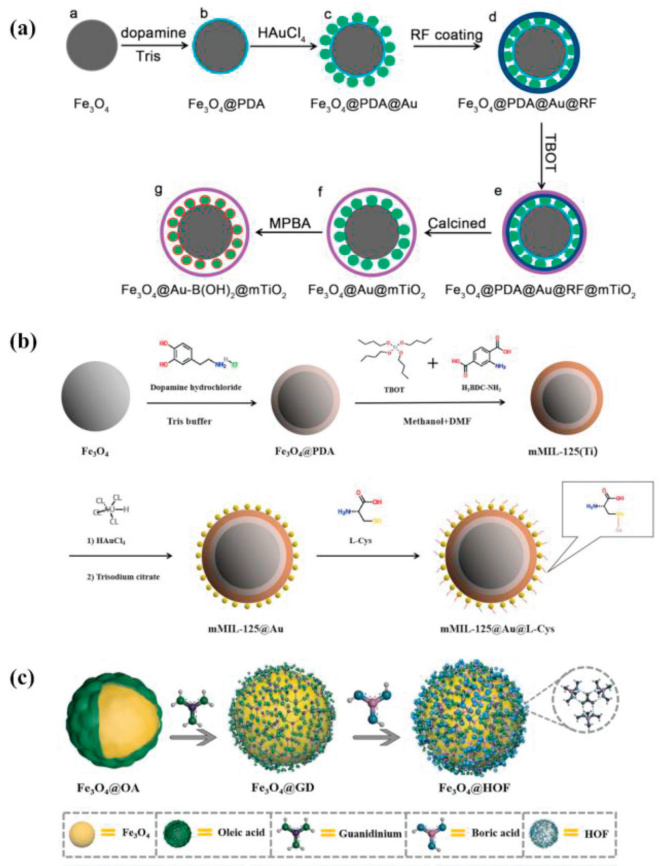

Fig. 6. (a) Preparation of Fe_3O_4@Au-B(OH)$_2$@mTiO_2. Reprinted with permission [139]. Copyright 2017, Elsevier B.V. (b) Synthesis of Fe_3O_4@PDA@MIL-125@Au@L-Cys. Reprinted with permission [145]. Copyright 2019, Elsevier B.V. (c) Synthesis of Fe_3O_4@HOF. Reprinted with permission [149]. Copyright 2024, Elsevier B.V.

saliva. The following year, Fe_3O_4@TiO_2-IDA was constructed by Sun *et al.* [143]. High sensitivity and selectivity were demonstrated in standard sample enrichment (β-casein 2.8×10^{-10} mol/L, HRP 0.9×10^{-10} mol/L, β-casein:BSA = 1:800, HRP:BSA = 1:100). In total, 550 phosphorylated peptides and 330 glycopeptides were identified in 100 μg mouse brain samples. Similarly, Xu *et al.* synthesized glucosamine-modified mSiO_2 (Fe_3O_4@TiO_2@mSiO_2-TSG) on Fe_3O_4@TiO_2 by a simple one-pot method [144]. The material possesses strong hydrophilicity, a suitable pore structure, a large specific surface area, strong magnetic responsiveness, and abundant metal oxide sites. Fe_3O_4@TiO_2@mSiO_2-TSG captured 94 endogenous glycopeptides and 164 endogenous phosphorylated peptides in 2 μL of undigested human saliva. In addition, Deng's group constructed novel nanomaterials with Au as the linker (denoted as Fe_3O_4@PDA@MIL-125@Au@L-Cy) (Fig. 6b) [145]. Outstanding sensitivity (0.1×10^{-9} mol/L) was demonstrated in the identification of HRP and β-casein digests. In total, 81 N-linked glycopeptides corresponding to 35 glycoproteins and 175 phosphopeptides corresponding to 55 phosphorylated proteins were identified in 100 mg of trypsin digested from human lens proteins, respectively.

As can be seen from the above two sections, the M-O portion of MOF materials can be enriched with phosphopeptides, and some MOFs have specific hydrophilic groups that can be enriched with glycopeptides. In other words, some MOF materials can do simultaneous enrichment. For example, Deng's group prepared Fe_3O_4@MIL-100(Fe) by layer-by-layer assembly (LBL) assembly method [146]. Zhang's group constructed bimetallic organic framework composites (named Fe_3O_4@SiO_2@(Zr-Ti-MOF)$_{10}$–NH_2) [147]. Both were prepared in a similar way, and both had good applications, especially in complex biological sample analysis. Fe_3O_4@MIL-100(Fe) captured 39 *N*-glycopeptides and 43 phosphopeptides in human saliva. A total of 141 N-linked glycopeptides corresponding to 127 glycoproteins and 918 phosphopeptides corresponding to 397 phosphoproteins were enriched and identified separately in tryptic digests from 0.5 mg of rat brain by Fe_3O_4@SiO_2@(Zr-Ti-MOF)$_{10}$–NH_2. Modification on the basis of MOFs can add the co-action of grafted substances. He *et al.* presented a magnetic cationic MOF composite (denoted as Fe_3O_4@ILI-01@Ti^{4+}) for the first time [148]. The reaction of Zn^{2+} as the center with 1,3-bis(4-carboxybutyl) imidazolium bromide (ILI) formed a MOF layer on the surface of Fe_3O_4 by autocoupling, and then Ti^{4+} was introduced to the material surface. The addition of Ti^{4+} increased the positive charge of the material and enhanced the enrichment effect on phosphorylated peptides (0.5×10^{-11} mol/L). The cation on ILI-01 has good hydrophilicity and shows a good enrichment performance for glycopeptides (0.1×10^{-11} mol/L). The high selectivity of the material is also attractive (1:5000 for β-casein:BSA and 1:500 for HRP:BSA, mass ratio).

In addition to COFs and MOFs, organic frameworks include hydrogen-bonded organic frameworks (HOFs). Xiong and coworkers constructed a magnetic biligand HOF (denoted as Fe_3O_4@HOF) (Fig. 6c) [149]. In their work, a cationic guanidino group and an anionic boronic acid group were used as ligands to enrich phosphopeptides and glycopeptides, respectively. In addition to the role of the guanidinium and boronic acid groups, the hydrogen bonding structure in the HOF material significantly enhanced its affinity for phosphopeptides and glycopeptides. Overall, the development of HOF materials shows its great potential in proteomics separation and analysis work and provides new means for future research.

5. Conclusions and perspective

In summary, MNMs have made great and effective progress in peptidomics in the last decade, and various strategies for capturing glycopeptides and phosphopeptides have been enriched and deeply applied. Magnetic adsorbents have greatly shortened the enrichment time and enhanced the enrichment performance of the materials. However, there is still room for further development of enrichment materials. For example, designing simpler and more environmentally friendly preparation processes, constructing functionalized probes with wider applicability, developing materials with higher sensitivity and specificity, and expanding the application and functionalization of magnetic materials beyond just Fe_3O_4. In addition, experimental conditions such as various buffers, enrichment time, and elution time also have a great influence on the enrichment results, and the optimal conditions for the experiments need to be found. Therefore, under the existing conditions, combining traditional methods with emerging strategies to construct novel functionalized MNMs, further deepening the enrichment mechanism, and obtaining more in-depth analyses in combination with MS is a major trend for subsequent research.

Biological samples such as skim milk, human saliva, serum, lens and mouse liver cell lysate, and brain digest are gradually becoming critical to examining the performance of these MNMs. At present, a large number of materials for peptide enrichment have been developed and used for further analysis. However, these materials are now being used to discover and characterize pre-existing or potential disease markers, but they are not yet in clinical use. This fact demonstrates their potential for application and provides new directions for peptidomics and disease. In view of the importance of glycoproteins and phosphoproteins in disease markers, their in-depth analysis is imperative. Based on the current state of development of one of the disease markers, it is still very challenging to screen and characterize them more intensively. Therefore, it is of great importance to develop novel mag-

netic functionalized materials to get more comprehensive enrichment and more in-depth analysis of disease markers for early diagnosis of diseases for future research. In addition, expand the sample size to obtain sufficient data to accurately analyze a particular disease marker. Furthermore, the tracking and quantification of potential disease markers and real-time monitoring of their concentration in the body are very important for clinical diagnosis and further determination of their potential as disease markers. Overall, there is still a huge potential for magnetic functionalized materials to be used in the discovery and analysis of disease markers.

Declaration of competing interest

The authors declare that they have no known competing financial interests or personal relationships that could have appeared to influence the work reported in this paper.

CRediT authorship contribution statement

Yimin Guo: Investigation, Writing – original draft. **Yiting Luo:** Investigation. **Shuwen Hua:** Formal analysis. **Chuan-Fan Ding:** Resources, Writing – review & editing. **Yinghua Yan:** Conceptualization, Writing – review & editing.

Acknowledgment

This work is supported by National Key Research and Development Program of China (No. 2023YFF0613402).

References

[1] Y.L. Li, N.R. Sun, X.F. Hu, Y. Li, C.H. Deng, TrAC Trends Anal. Chem. 120 (2019) 115658.
[2] Y.J. Chen, H.L. Chen, C.J. Yang, et al., Chin. Chem. Lett. 34 (2023) 107352.
[3] B.C. Wang, Z.H. Xie, C.F. Ding, C.H. Deng, Y.H. Yan, TrAC Trends Anal. Chem. 158 (2023) 116881.
[4] S.W. Hua, B. Wang, C.F. Ding, Y.H. Yan, Talanta 266 (2023) 125139.
[5] Y.F. Lin, C.R. Du, H.M. Ying, et al., Anal. Chim. Acta 1287 (2024) 342058.
[6] S. Zhao, W.Y. Hu, D.T. Zhang, X.Y. Wang, G.S. Guo, Microchem. J. 195 (2023) 109423.
[7] A.K. Swaroop, P.K.K. Namboori, M. Esakkimuthukumar, et al., Comput. Biol. Med. 163 (2023) 107231.
[8] B. Wang, X.Y. Zhang, S.W. Hua, C.F. Ding, Y.H. Yan, Microchim. Acta 191 (2024) 26.
[9] L.C. Chan, C.W. Li, W.Y. Xia, et al., J. Clin. Invest. 129 (2019) 3324–3338.
[10] E. Valdes-Marquez, R. Clarke, M. Hill, H. Watkins, J.C. Hopewell, Eur. J. Prev. Cardiol. 30 (2023) 583–591.
[11] J.K. Chen, B. Wang, Y.T. Luo, et al., Talanta 264 (2023) 124771.
[12] N.R. Sun, H. Wu, X.Z. Shen, C.H. Deng, Adv. Funct. Mater. 29 (2019) 1900253.
[13] L.L. Kong, F.Z. Li, W. Fang, et al., Anal. Chem. 95 (2023) 11326–11334.
[14] N.R. Sun, H.L. Yu, H. Wu, X.Z. Shen, C.H. Deng, TrAC Trends Anal. Chem. 135 (2021) 116168.
[15] Y.J. Chen, T.C. Yen, Y.H. Lin, et al., Anal. Chem. 93 (2021) 15931–15940.
[16] L.P. Liu, S.X. Jin, P.C. Mei, P. Zhou, Talanta 203 (2019) 58–64.
[17] Z.X. Li, Q. Wang, J.W. Mao, et al., Anal. Chim. Acta 1142 (2021) 48–55.
[18] A. Goumenou, N. Delaunay, V. Pichon, Front. Mol. Biosci. 8 (2021) 746822.
[19] D.Q. Wang, J.F. Huang, L.J. Li, ACS Appl. Mater. Interfaces 15 (2023) 47893–47901.
[20] X.Y. Zhou, H.Y. Zhang, L. Wang, L.T. Lv, R.A. Wu, Analyst 148 (2023) 1483–1491.
[21] D.D. Jiang, X.Q. Li, J.T. Ma, Q. Ji, Talanta 180 (2018) 368–375.
[22] J. Li, J.H. Huang, Y.J. Jiang, L.M. Wu, Y.H. Deng, Adv. Funct. Mater. 33 (2023) 2212317.
[23] Q. Yue, J.G. Sun, Y.J. Kang, Y.H. Deng, Angew. Chem. Int. Ed. 59 (2020) 15804–15817.
[24] C.Y. Yuan, X.Q. Wang, X.Y. Yang, et al., Chin. Chem. Lett. 32 (2021) 2079–2085.
[25] Y. Zhang, Q. Yue, M.M. Zagho, et al., ACS Appl. Mater. Interfaces 11 (2019) 10356–10363.
[26] Y.M. Guo, S.W. Hua, B.C. Wang, et al., Analyst 148 (2023) 5864–5872.
[27] Y.T. Luo, B.C. Wang, L.H. Yi, et al., TrAC Trends Anal. Chem. 167 (2023) 117234.
[28] H.W. Zheng, H. Lin, X.F. Chen, et al., TrAC Trends Anal. Chem. 129 (2020) 115952.
[29] H. Qi, L.Y. Jiang, Q. Jia, Chin. Chem. Lett. 32 (2021) 2629–2636.
[30] Y.A. Chang, D. Zhu, W.J. Duan, et al., Int. J. Biol. Macromol. 193 (2021) 1541–1550.
[31] X.Y. Feng, C.H. Deng, M.X. Gao, X.M. Zhang, Anal. Bioanal. Chem. 410 (2018) 989–998.
[32] J. Wei, Y. Ren, W. Luo, et al., Chem. Mater. 29 (2017) 2211–2217.
[33] Z.X. Xu, H.L. Chen, H.M. Chu, et al., Chin. Chem. Lett. 34 (2023) 107829.
[34] W.D. Ma, C. Zhong, J. Lin, et al., Chin. Chem. Lett. 33 (2022) 5174–5179.
[35] H.M. Chen, Y.L. Li, H. Wu, N.R. Sun, C.H. Deng, ACS Sustain. Chem. Eng. 7 (2019) 2844–2851.
[36] Z.X. Xu, Y.L. Wu, Z.Q. Deng, et al., Talanta 234 (2021) 122713.
[37] H. Qi, Z. Li, H.J. Zheng, L. Fu, Q. Ji, Chin. Chem. Lett. 30 (2019) 2181–2185.
[38] P. Su, M. Li, X. Li, et al., J. Chromatogr. A 1667 (2022) 462869.
[39] W.W. Huan, J.S. Zhang, H. Qin, et al., Nanoscale 11 (2019) 10952–10960.
[40] N. Zhang, X.F. Hu, H.L. Chen, C.H. Deng, N.R. Sun, Chem. Commun. 57 (2021) 6249–6252.
[41] L.H. Yi, Y.F. Shao, M.Y. Fu, et al., J. Chromatogr. A 1669 (2022) 462929.
[42] B.F. Zhao, W.H. Xu, J.T. Ma, Q. Jia, Chin. Chem. Lett. 34 (2023) 107498.
[43] J.Y. Lu, J.Y. Luan, Y.J. Li, et al., J. Chromatogr. A 1615 (2020) 460754.
[44] X.W. Li, H.Y. Zhang, N. Zhang, et al., ACS Sustain. Chem. Eng. 7 (2019) 11511–11520.
[45] L. Ma, C.R. Su, X.Y. Li, et al., Food Hydrocoll. 148 (2024) 109410.
[46] B. Wang, X.Y. Zhang, B.C. Wang, et al., Microchim. Acta 190 (2023) 399.
[47] N. Li, T.C. Zhang, W.H. Xue, et al., Sep. Purif. Technol. 330 (2024) 125206.
[48] C.F. Bi, Y.L. Liang, L.J. Shen, et al., ACS Omega 3 (2018) 1572–1580.
[49] L. Zhang, X.F. Yue, N. Li, et al., Anal. Chim. Acta 1088 (2019) 63–71.
[50] Y.L. Li, J.W. Wang, N.R. Sun, C.H. Deng, Anal. Chem. 89 (2017) 11151–11158.
[51] X.F. Hu, Y.L. Wu, C.H. Deng, Microchim. Acta 187 (2020) 616.
[52] N.R. Sun, H. Wu, H.M. Chen, X.Z. Shen, C.H. Deng, Chem. Commun. 55 (2019) 10359–10375.
[53] Z.Z. Lai, M. Zhang, J.Y. Zhou, et al., Analyst 146 (2021) 4261–4267.
[54] Y.J. Chen, Z.C. Xiong, L.Y. Zhang, et al., Nanoscale 7 (2015) 3100–3108.
[55] B. Jiang, Q. Wu, N. Deng, et al., Nanoscale 8 (2016) 4894–4897.
[56] J.W. Wang, J.Z. Yao, N.R. Sun, C.H. Deng, J. Chromatogr. A 1512 (2017) 1–8.
[57] Q.J. Liu, N.R. Sun, C.H. Deng, TrAC Trends Anal. Chem. 110 (2019) 66–80.
[58] C. Liu, J. Wang, J.J. Wan, C.Z. Yu, Coord. Chem. Rev. 432 (2021) 213743.
[59] M.H. Wang, M.Y. Hu, Z.Z. Li, et al., Biosens. Bioelectron. 142 (2019) 111536.
[60] C.X. Zhang, C.F. Xie, Y.Y. Gao, et al., Angew. Chem. Int. Ed. 61 (2022) e202204108.
[61] C.J. Hu, J.B. Chen, H.Q. Zhang, et al., Microchem. J. 180 (2022) 107595.
[62] Y.Q. Xie, C.H. Deng, Y. Li, J. Chromatogr. A 1508 (2017) 1–6.
[63] J.X. Wang, X.M. Wang, J. Li, et al., J. Mater. Chem. B 10 (2022) 2011–2018.
[64] Q.Y. Gu, H.L. Zhao, T.Y. Zhu, et al., Talanta 267 (2023) 125165.
[65] X.J. Ma, T.F. Scott, Commun. Chem. 1 (2018) 98.
[66] H.P. Wang, F.L. Jiao, F.Y. Gao, et al., J. Mater. Chem. B 5 (2017) 4052–4059.
[67] Y. Zhang, M. Yu, C. Zhang, et al., Chem. Commun. 51 (2015) 5982–5985.
[68] Q.Q. Zhang, Y.Y. Huang, B.Y. Jiang, et al., Anal. Chem. 50 (2018) 7357–7363.
[69] J. Su, X.W. He, L.X. Chen, Y.K. Zhang, Talanta 180 (2018) 54–60.
[70] X.T. Xue, R. Lu, M. Liu, et al., Analyst 144 (2019) 641–648.
[71] S.T. Li, Y.R. Qin, G.Q. Zhong, et al., ACS Appl. Mater. Interfaces 10 (2018) 27612–27620.
[72] J.Y. Luan, X.K. Zhu, L.C. Yu, et al., Talanta 251 (2023) 123772.
[73] Z.Y. Guo, Y. Sun, L.R. Zhang, et al., J. Colloid Interface Sci. 615 (2022) 597–605.
[74] X.Y. Sun, R.T. Ma, J. Chen, Y.P. Shi, Microchim. Acta 185 (2018) 12.
[75] J.J. Shu, W.L. Xiong, R. Zhang, et al., Talanta 253 (2022) 123956.
[76] Y. Chen, H.Q. Qin, X.Y. Yue, et al., Anal. Chem. 93 (2021) 16618–16627.
[77] Q.C. Cao, C. Ma, H.H. Bai, et al., Analyst 139 (2014) 603–609.
[78] L.T. Liu, M. Yu, Y. Zhang, C.C. Wang, H.J. Lu, ACS Appl. Mater. Interfaces 6 (2014) 7823–7832.
[79] B. Jiang, Q. Wu, L.H. Zhang, Y.K. Zhang, Nanoscale 9 (2017) 1607–1615.
[80] J.X. Peng, H. Niu, H.Y. Zhang, et al., ACS Appl. Mater. Interfaces 15 (2018) 32613–32621.
[81] C.M. Potel, M.H. Lin, A.J.R. Heck, S. Lemeer, Mol. Cell. Proteomics 17 (2018) 1028–1034.
[82] Q. Wang, X.M. He, X. Chen, et al., J. Chromatogr. A 1499 (2017) 30–37.
[83] M.M. Zhang, H. Wang, R. Bhandari, Q.H. Pan, F.Y. Sun, Anal. Bioanal. Chem. 413 (2021) 2893–2901.
[84] Q.J. Liu, N.R. Sun, M.X. Gao, C.H. Deng, ACS Sustain. Chem. Eng. 6 (2018) 4382–4389.
[85] H.M. Chu, H.Y. Zheng, A.Z. Miao, C.H. Deng, N.R. Sun, Chin. Chem. Lett. 34 (2023) 107716.
[86] W.K. Zhu, D.T. Yang, A.M. Gronenborn, J. Am. Chem. Soc. 145 (2023) 4564–4569.
[87] K.N. Zhang, Y. Hao, D.H. Hu, et al., J. Chromatogr. A 1659 (2021) 462648.
[88] C.H. Zhang, Y.N. Pan, Y.M. Zhao, et al., Anal. Chim. Acta 1186 (2021) 339099.
[89] B. Liu, B.C. Wang, Y.H. Yan, K.Q. Tang, C.F. Ding, Microchim. Acta 188 (2021) 32.
[90] Z.X. Xu, Y.L. Wu, H. Wu, N.R. Sun, C.H. Deng, Anal. Chim. Acta 1146 (2021) 53–60.
[91] X.N. Sun, X.D. Liu, J.A. Feng, et al., Anal. Chim. Acta 880 (2015) 67–76.
[92] J.B. Jiang, X.N. Sun, X.J. She, et al., Microchim. Acta 185 (2018) 309.
[93] H.Z. Lin, C.H. Deng, Talanta 149 (2016) 91–97.
[94] J.B. Jiang, X.N. Sun, Y. Li, C.H. Deng, G.L. Duan, Talanta 178 (2018) 600–607.
[95] J.S. Harrington, S.W. Ryter, M. Plataki, D.R. Price, A.M.K. Choi, Physiol. Rev. 103 (2023) 2349–2422.
[96] L.Y. Zhang, Q. Zhao, Z. Liang, et al., Chem. Commun. 48 (2012) 6274–6276.
[97] L.Y. Zhang, Z. Liang, L.H. Zhang, Y.K. Zhang, S.J. Shao, Anal. Chim. Acta 900 (2015) 46–55.
[98] J. Su, X.W. He, L.X. Chen, Y.K. Zhang, ACS Sustain. Chem. Eng. 6 (2018) 2188–2196.
[99] X.S. Li, L.D. Xu, G.T. Zhu, B.F. Yuan, Y.Q. Feng, Analyst 137 (2012) 959–967.

[100] Q.W. Yu, X.S. Li, Y.S. Xiao, et al., J. Chromatogr. A 1365 (2014) 54–60.
[101] D.D. Jiang, S. Lv, X. Han, et al., Microchim. Acta 188 (2021) 327.
[102] Y.T. He, S.S. Zhang, C. Zhong, et al., Talanta 235 (2021) 122789.
[103] J.Z. He, J.J. Li, J.L. Zhang, et al., Carbon 214 (2023) 118266.
[104] N.K. Chen, Y.Y. Xiao, C. Wang, J.H. He, N.N. Song, ACS Appl. Mater. Interfaces 15 (2023) 48529–48542.
[105] Y. Wang, Y.Y. Wei, P.C. Gao, et al., ACS Appl. Mater. Interfaces 13 (2021) 11166–11176.
[106] R.F. Gao, J. Li, R. Shi, et al., J. Mater. Sci. Technol. 59 (2020) 234–242.
[107] X.Q. Chen, S.Y. Li, X.X. Zhang, Q.H. Min, J.J. Zhu, Nanoscale 7 (2015) 5815–5825.
[108] Q.H. Min, S.Y. Li, X.Q. Chen, et al., ACS Appl. Mater. Interfaces 7 (2015) 9563–9572.
[109] D.S. Roberts, B.F. Chen, T.N. Tiambeng, et al., Nano Res. 12 (2019) 1473–1481.
[110] X.Y. Long, J.Y. Li, D. Sheng, H.Z. Lian, Talanta 166 (2017) 36–45.
[111] H.L. Chen, Y. Qi, C.Y. Yang, et al., ACS Nano 17 (2023) 23924–23935.
[112] J.Y. Li, X.Y. Long, D. Sheng, H.Z. Lian, Talanta 208 (2020) 120437.
[113] M.Y. Wang, C.H. Deng, Y. Li, X.M. Zhang, ACS Appl. Mater. Interfaces 6 (2014) 11775–11782.
[114] D.D. Jiang, S.Q. Lv, R.X. Qi, J.H. Liu, L.M. Duan, J. Chromatogr. A 1678 (2022) 463374.
[115] Y.Y. Hong, Q.L. Zhan, C.L. Pu, et al., Talanta 187 (2018) 223–230.
[116] Y.Y. Hong, C.L. Pu, H.L. Zhao, et al., Nanoscale 9 (2017) 16764–16772.
[117] Y.L. Li, L.L. Liu, H. Wu, C.H. Deng, Anal. Chim. Acta 1079 (2019) 111–119.
[118] A. Ostovan, M. Arabi, Y.Q. Wang, et al., Adv. Mater. 34 (2022) 2203154.
[119] X.W. Fang, Z.D. Wang, N.R. Sun, C.H. Deng, Talanta 223 (2021) 122143.
[120] Y. Chen, D.J. Li, Z.J. Bie, X.P. He, Z. Liu, Anal. Chem. 88 (2016) 1447–1454.
[121] X.W. Fang, Z.D. Wang, N.R. Sun, C.H. Deng, Talanta 226 (2021) 122143.
[122] Q.S. Liu, K.N. Zhang, Y.H. Jin, et al., Talanta 186 (2018) 346–353.
[123] N. Zhang, N.R. Sun, C.H. Deng, Chem. Commun. 56 (2020) 13999–14002.
[124] R.L. Xiao, Y.N. Pan, J. Li, L.Y. Zhang, W.B. Zhang, J. Chromatogr. A 1601 (2019) 45–52.
[125] S. Yan, B. Luo, J. Cheng, et al., J. Mater. Chem. B 10 (2022) 9671–9681.
[126] N. Zhang, T. Huang, P.S. Xie, et al., ACS Appl. Mater. Interfaces 14 (2022) 39364–39374.
[127] S. Yan, B. Luo, J. He, F. Lan, Y. Wu, J. Mater. Chem. B 9 (2021) 1811–1820.
[128] H. Qi, G. Chen, Q. Jia, Talanta 247 (2022) 123563.
[129] J.X. Peng, H.Y. Zhang, X. Li, et al., ACS Appl. Mater. Interfaces 8 (2016) 35012–35020.
[130] J.Q. Zhou, Y.L. Liang, X.W. He, L.X. Chen, Y.K. Zhang, ACS Sustain. Chem. Eng. 5 (2017) 11413–11421.
[131] W. Gao, F. Zhang, S. Zhang, J.Y. Li, H.Z. Lian, Sep. Purif. Technol. 305 (2023) 122426.
[132] D.S. Yang, X.Y. Ding, H.P. Min, et al., J. Chromatogr. A 1505 (2017) 56–62.
[133] J.W. Wang, Z.D. Wang, N.R. Sun, C.H. Deng, Microchim. Acta 186 (2019) 236.
[134] B. Luo, X.X. Zhou, P.P. Jiang, et al., J. Mater. Chem. B 6 (2018) 3969–3978.
[135] D.D. Jiang, L.M. Duan, Q. Jia, J.H. Liu, Anal. Chim. Acta 1136 (2020) 25–33.
[136] H. Qi, Z. Li, H.J. Zheng, Q. Jia, Anal. Chim. Acta 1157 (2021) 338383.
[137] L.Z. Yu, J. He, S. Yan, et al., ACS Sustain. Chem. Eng. 10 (2022) 2494–2508.
[138] D.P. Xu, M.X. Gao, C.H. Deng, X.M. Zhang, Anal. Bioanal. Chem. 408 (2016) 5489–5497.
[139] D.P. Xu, G.Q. Yan, M.X. Gao, C.H. Deng, X.M. Zhang, Talanta 166 (2017) 154–161.
[140] Z.D. Wang, J.W. Wang, N.R. Sun, C.H. Deng, Anal. Chim. Acta 1067 (2019) 1–10.
[141] Y.Y. Hong, H. Zhao, C.L. Pu, et al., Anal. Chem. 90 (2018) 11008–11015.
[142] N.R. Sun, J.W. Wang, J.Z. Yao, H.M. Chen, C.H. Deng, Microchim. Acta 186 (2019) 159.
[143] N.R. Sun, H. Wu, X.Z. Shen, Microchim. Acta 187 (2020) 3.
[144] Z.X. Xu, Y.L. Wu, X.F. Hu, C.H. Deng, N.R. Sun, Chin. Chem. Lett. 33 (2022) 4695–4699.
[145] Y.L. Wu, Q.J. Liu, C.H. Deng, Anal. Chim. Acta 1061 (2019) 110–121.
[146] Y.L. Wu, Q.J. Liu, Y.Q. Xie, C.H. Deng, Talanta 190 (2018) 298–312.
[147] Y.N. Pan, C.H. Zhang, R.L. Xiao, L.Y. Zhang, W.B. Zhang, Anal. Chim. Acta 1158 (2021) 338412.
[148] H. Qi, Z. Li, J.T. Ma, Q. Jia, J. Mater. Chem. B 10 (2022) 3560–3566.
[149] F.F. Xiong, T. Zhang, J.T. Ma, Q. Jia, Talanta 266 (2024) 125068.